MENTATION PAGE

Form Approved
OMB No 0704-0188

REPORT DATE	3. REPORT TYPE AND DATES COVERED
15 March 91	Final, period 1 6/7/90 to 6/3/91

4. TITLE AND SUBTITLE
Reaction Rate Engineering Models of Fatique Crack Growth

5. FUNDING NUMBERS
F49620-90-C-0059

6. AUTHOR(S)
F. Kozin & J.L. Bogdanoff

7. PERFORMING ORGANIZATION NAME(S) AND ADDRESS(ES)
Kozin Bogdanoff & Assoc., Inc.
P.O. Box 2372
West Lafayette, IN 47906

8. PERFORMING ORGANIZATION REPORT NUMBER
AFOSR-TR- 91 0514

9. SPONSORING MONITORING AGENCY NAME(S) AND ADDRESS(ES)
AFOSR/XOT (SBIR Program Manager)
Bldg. 410, RM A-119
Bolling AFB, DC 20332-6448

10. SPONSORING MONITORING AGENCY REPORT NUMBER
F49620-90-C-0059

11. SUPPLEMENTARY NOTES

12a. DISTRIBUTION AVAILABILITY STATEMENT
Unrestricted

12b. DISTRIBUTION CODE

13. ABSTRACT (Maximum 200 words)

A macro model is presented of fatigue cracks growth (FCG) in a thin center crack panel of polycrystalline ductile metal subject to an axial periodically varying tensile load. The macro model is based upon a fundamental micro result from reaction rate theory. The deterministic version of this model applies to the mean time to reach a given crack length. Variability is introduced at the macro level to produce a probabilistic version. The parameters of this physically based model are directly related to the physical properties of the material, the temperature T, and the load. The form of the periodic load and T are important quantities in predicting crack growth.

Analysis of FCG data for periodically varying loads reveals that three material parameters are required. The minimum amount testing required for predictive purposes is also discussed as is an interesting method for accelerating tests.

Because of the physical basis of the model, it provides new insight into the FCG process.

14. SUBJECT TERMS
Micro, Macro, Reaction rate, Fatigue crack growth, minimize and accelerate testing, Probabilistic.

15. NUMBER OF PAGES

16. PRICE CODE

17. SECURITY CLASSIFICATION OF REPORT	18. SECURITY CLASSIFICATION OF THIS PAGE	19. SECURITY CLASSIFICATION OF ABSTRACT	20. LIMITATION OF ABSTRACT
Unclassified	Unclassified	Unclassified	None

Reaction Rate Engineering Models

of

Fatigue Crack Growth

AFOSR Contract No. F49620-90-C-0059

Final Report

by

J. L. Bogdanoff

T. T. Soong

of

Kozin Bogdanoff & Associates Inc.

P. O. Box 2372

West Lafayette, IN 47906

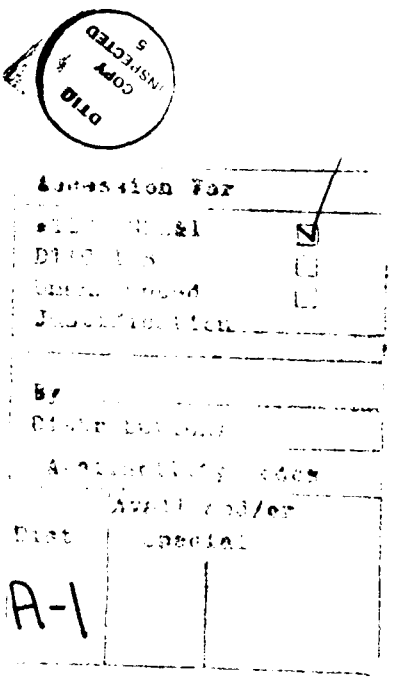

March 5, 1991

Table of Contents

1. Engineering Significance of Phase I Study

In comparison with other existing fatigue crack growth models, the present model offers the following features of engineering significance.

a) The mean fatigue crack growth model is developed based on fundamental results provided by physical theory. The parameters of the model thus have physical significance and they provide new insight into the crack growth process.

b) The model parameters are directly related to the simple harmonic tensile load and the temperature. Hence, test data under varying loading conditions and varying temperatures can be used for parameter estimation. Furthermore, validation of the model using existing test data shows that the crack growth behavior can be reliably predicted based on two or at most three suitably chosen tests. Considerable savings in cost and time associated with testing, data collection and data analysis can thus be realized.

c) The model indicates that testing time can be shortened by simply increasing the temperature with the same loads. This procedure eliminates the load interaction problem when using the standard method of accelerating fatigue and FCG tests by increasing the loads.

d) Inherent variabilities in material behavior, load, temperature, and environment can be incorporated into the mean model.

From an engineering viewpoint, these features represent an important improvement over existing and more phenomenologically based models. It is proposed that further development of this model and its implementational issues can be addressed in Phase II.

2. Summary of Work Done in Phase I Study

The following tasks were specified in the Phase I Proposal and in Contract F49620-90-C-0059 funded by AFOSR:

Task i) A deterministic macro model of damage accumulation for fatigue crack growth (FCG) will be constructed from the micro theory.

Task ii) Identify the parameters in the macro model with physical and material properties of engineering significance to determine which must be estimated by testing and which can be estimated from known material properties.

Task iii) Four sets of existing data on FCG will be used to explore the parameter estimation problem in order to determine the minimum amount of testing needed to characterize a component for prediction purposes.

Task iv) Determine how variability is to be included in the deterministic engineering model so that the inherent probabilistic distributions present in the phenomenon can be included.

These tasks and more were completed.

Let us summarize briefly how these tasks were accomplished, and what was learned in the process. Details are provided in the references 1 and 2.

Figure 1 shows the crack plane on one-half a thin center crack panel under axial tensile load; a_o is the initial one-half crack length, a is the current one-half crack length, and ξ is a generic point in the intake portion of the one-half crack plane. Let us introduce some notation.

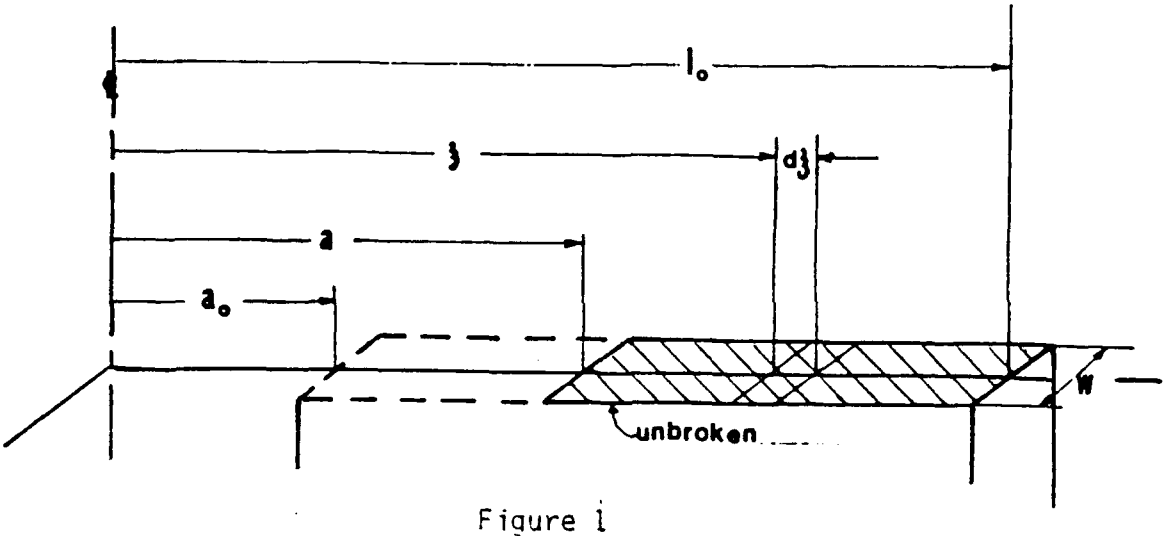

Figure 1

a_j = 1/2 the j^{th} crack length considered, j = 1 , ..., n,

$y_j = a_j/\ell_o$, ℓ_o = 1/2 the panel width,

$\Delta a_j = a_j - a_{j-1}$, $\Delta y_j = \Delta a_j/\ell_o$,

w = panel thickness,

s_o = far field axial tensile stress,

$= \bar{s}_o + \Delta s\ h(\omega t) > 0$

$h(\tau)$ = periodic function on $(0,2\pi)$, $|h(\tau)| \leq 1$, mean $h(\tau) = 0$

T = absolute temperature (Kelvin),

t_j = mean time to reach a_j, $\Delta t_j = t_j - t_{j-1}$.

$\bar{y}_j = (y_j + y_{j-1})/2$.

Task i): A deterministic macro model of damage accumulation for fatigue crack growth (FCG) will be constructed from micro (reaction rate) theory.

A deterministic macro model of FCG in a thin center crack panel of polycrystaline ductile metal under an axial tensile load with a periodic time variation is produced from a micro result provided by reaction rate theory. Specifically, the macro model gives

$$\Delta t_j = f(\Delta y_j, \bar{y}_j, \varepsilon, z; \bar{s}_o, \Delta s, h(\tau), T; \Delta G^+, \beta_j \text{ or } \lambda_j/\nu \ ,$$

where $\beta_j = \lambda_j/\nu kT$ is the growth control parameter, k = Boltzmann's constant, h = Planck's constant, and ν = mean number of bonds per unit area. Only one damage accumulation observable, namely y, is present, although other possibilities exist, ε and z are geometrical constants that refer to the normal stress in distribution $s(\xi)$ on $(a \leq \xi \leq \ell_o)$; and T is assumed constant. We note that to predict Δt_j

the geometrical quantities Δy_j, $\bar{y}_j$, ε, z
must be selected,

the environmental factors $\bar{s}_o$, Δs , $h(\tau)$, T
must be obtained from the operating conditions, and

the material parameters ΔG^+, β_j or λ_j/ν
must be estimated.

The model is new. It is based upon physical theory, and it explicitly contains qualities of engineering interest. Details of the derivation

are given in Sections 2, 3, and 4 in Reference [1] and in Section 2 in [2]. Thus Task i) is completed for one specimen geometry and load.

Task ii): Identify the parameters in the macro model with physical and material properties of engineering significance to determine which must be estimated by testing and which can be estimated from known material properties.

The macro deterministic model contains explicitly the physical (environmental) parameters $\bar{s}_o$, Δs, $h(\tau)$, and T that are of direct engineering significance. $\bar{s}_o$, Δs, and $h(\tau)$ describe the load considered here, and are known once the load is specified. T is the temperature of the component or specimen and is known once the environment is specified. We usually assume T is constant, although this is not necessary; we also assume there are no chemical agents in the atmosphere. It turns out from our studies that $h(\tau)$ and T are more important in the estimation of Δt_j than previously thought.

The macro model also contains the material parameters ΔG^+ and β_j. ΔG^+ is a Gibbs free energy; it is a thermodynamic property, and it only depends on the material composition; it can be estimated for metals from known information on the heat of sublimation of the metalic elements and the composition. β_j not only depends on the material composition but it also depends on how the material is formed (cast, forged, annealed, etc.) into components. β_j is correlated with microscopic material properties. β_j must be estimate from test data at present. Details are given in Sections 2, 3, and 4 in [1], and in Section 2 in [2]. Task ii) is thus accomplished.

Task iii): Four sets of existing data on FCG will be used to explore the parameter estimation problem in order to determine the minimum amount of testing needed to characterize a component for predictive purposes.

Actually, six sets of FCG data were used to explore the parameter estimation problem. The parameter we estimate is $\beta_j \bar{s}_o'$, where $\bar{s}_o' = \bar{s}_o + \Delta s$. In each set, it was found that $\beta_j \bar{s}_o'$ could be expressed in terms of a linear expression in β_o, c and y: $\beta_j \bar{s}_o' = \beta_o \bar{s}_o'(1-c\bar{y}_j)$. This means there are three material parameters ΔG^+, β_o, c of which β_o and c must be estimated from test data. It was found that β_o depends on the load whereas c does not. β_o depends on T in a known manner but c does not seem to. Tests at three different loads are the maximum required in order to be able to estimate β_o as a function of the load. Then, it is possible to predict the mean time t_j to reach the crack length a_j for a range of loads.

We also found that it is possible to accelerate tests by increasing T. Thus, we have found the minimum amount of testing required to characterize a component for predictive purposes.

For details, see Sections 3, 4, and 7 in [2] and Sections 5 and 6 in [1]. We thus have completed Task iii).

Task iv): Determine how variability is to be included in the deterministic engineering model so that the inherent probabilistic distributions present in the phenomenon can be included.

We have found that variability can be introduced at the macro level in the deterministic model by assuming that the work done in bond breaking on the Δy_j interval, $\beta_j \bar{s}_o'$, has a random factor Q_j. The data sets are employed to estimate the moments and distributions of the Q_j. What is remarkable is that the distributions of the standardized Q_j are very

close to one another and do not seem to depend on the load or interval length. We have no explanation for this remarkable fact based on this macro method for introducing variability. However, this approach to variability does not enable us to determine if the distributions of the Q_j depend on T. The tests needed for parameter estimation in the deterministic model suffice to estimate the parameters in the probabilistic model for predictive purposes providing T does not change.

See Sections 5 and 6 in [2] for details. Task iv) is thus completed.

Persual of [1] and [2] makes clear that more must be done to validate the current model, to further develop the current model so that, for example, it applies to different crack geometries and loads, and to remove some of the restrictive assumptions employed in the current model.

References

1. Kozin, F. and Bogdanoff, J. L., "Cumulative Damage for Mean Fatigue Crack Growth Based on the Kinetic Theory of Thermally Activated Fracture," Engrg. Fract. Mech., Vol. 37, No. 5, pp. 995-1010, 1990, (See Appendix I).
2. Kozin, F. and Bogdanoff, J. L., "Cumulative Damage Model for Fatigue Crack Growth Based on Reaction Rate Theory," submitted to Engrg. Fract. Mech. for publication (see Appendix II).

APPENDIX I

Engineering Fracture Mechanics Vol. 37, No. 5, pp. 995–1010, 1990
Printed in Great Britain.

CUMULATIVE DAMAGE MODEL FOR MEAN FATIGUE CRACK GROWTH BASED ON THE KINETIC THEORY OF THERMALLY ACTIVATED FRACTURE

F. KOZIN† and J. L. BOGDANOFF‡

†Polytechnic University Route 110, Farmingdale, NY 11735, U.S.A.
‡School of Aeronautics and Astronautics, Purdue University, W. Lafayette, IN 47907, U.S.A.

Abstract—The objective of this paper is to show how the physical concepts due to Tobolsky–Eyring for the description of atomic (micro) bond fracture can be extended to the macro problem of mean fatigue crack growth which is of engineering interest. The parameters of the model have physical meaning. Parameter estimation is studied with the aid of four data sets on fatigue crack growth. Because of the fundamental physical concepts employed, the model provides new insights into the fatigue crack growth process.

1. INTRODUCTION

THE PURPOSE of this paper is to present an initial study of a mean fatigue crack growth (FCG) model based upon the kinetic theory of thermally activated atomic bond fracture due to Tobolsky–Eyring[1].

We start from a basic expression for the mean rate of single atomic bond breaking that has its origin in the statistical theory of thermally activated bond fracture. A brief discussion of the applicability of the expression is given.

From the basic expression, which applies at the micro level, we derive a differential equation for mean crack growth in a center crack panel or WOL specimen under tensile load that applies at the macro level. This is a major contribution of the paper.

Employing certain simplifying assumptions, we then obtain a formula for mean crack growth whose parameters have physical meaning. Some of these parameters are directly related to the load; others refer to material properties. One parameter can frequently be estimated from tabulated physical data; however, the other unknown parameters must be estimated from experimental data.

The statistical analysis available for four sets of high replication data provide the basic information on mean crack growth as a function of time with which the remaining parameters can be estimated. These estimates provide new insights into the crack growth process under simple harmonic tensile loading, including the effect of load shedding. This is a second major contribution.

A third major contribution is the fact that the mean model presented can predict mean fatigue crack growth behavior in a component under arbitrarily varying simple harmonic tensile loading at any temperature based on two or at most three suitably chosen tests.

Finally, we discuss the results, and offer suggestions for future study part of which will be presented in a subsequent paper.

We wish to emphasize at this point that the model we develop is different from other mean models. We are concerned with cumulative damage in which crack length is a macro observable and a measure of macro damage accumulation, starting from a basic expression for atomic bond breaking which applies at the micro level. Earlier models do not have this focus. Further, this model has no contact with the concepts usually employed in fracture mechanics.

2. BOND BREAKING WITH A SINGLE ENERGY BARRIER AND NO BOND MENDING

The mean rate, κ_b, of single atomic bond breaking, when there is only a single energy barrier, no bond mending, and a tensile external force present, is, according to physical theory as developed by Tobolosky–Eyring[1] (see also p. 338 in ref. [2]), given by

$$\kappa_b = \frac{kT}{h} e^{-\frac{\Delta G^* - \gamma f}{kT}}, \tag{1}$$

where

k = Boltzmann's constant,
T = absolute temperature,
h = Planck's constant,
ΔG^* = free energy of activation,
λ = average distance over which force acts in bond breaking,
f = average force acting on a single bond during bond breaking.

Let us briefly discuss the meanings of the last three quantities, and the form of the exponent in eq. (1).

ΔG^* and λ are material parameters. Tobolsky–Eyring[1, 2] interpret the free energy ΔG^* as the height of the single energy barrier that must be overcome in order to break a bond. ΔG^* also may be thought of (Zhurkov[3]) as the binding energy of atoms in metals and the energy of breakage of the chemical bonds in chain macro molecules in polymers.

The atomic bond force f depends on the external tensile force acting. We shall assume below that f may be approximated by a term proportional to the stress, as was done in refs [1–3]. Thus, eq. (1) says, as noted in ref. [4], that "the free energy of activation is, in effect, reduced linearly (in stress) in a manner identical to that proposed by Eyring[5] for molecular interpretation of liquid viscosity". Further, the extensive experimental studies of Zhurkov[3] also demonstrate that a linear dependence on stress in the exponent of eq. (1) is required to describe his data on time to failure under constant stress.

The second material parameter is λ. λ is the average distance over which the force f acts during bond breaking. In ref. [4], it is regarded as the mean separation between the equilibrium positions of minimum force potential. It is clear from the form of the exponent in eq. (1) that λ is inversely proportional to the strength of the material. λ will be influenced by how the material is formed into components, and by work hardening or softening. Zhurkov[3] (replace his γ by λ) gives some very interesting observations on the meaning of this parameter. For example, a direct correlation has been found between λ and the disorientation of the structure; the more disorientated the structure in a metal, i.e. the higher the dislocation density at the slip planes, the smaller the strength coefficient λ, and hence the higher the metal strength, etc. Thus, λ is an important parameter.

In all events, the form of eq. (1) has substantial support in experiments on a variety of materials including polycrystalline metals and polymers.

Equation (1) applies at the micro scale; i.e. it gives the mean rate of single bond breaking under the conditions stated. Our concern with failure (fracture) is at the macro level. Thus, it is necessary to derive from eq. (1) a macro model of failure. It is worth noting at this point that a comparison of several macro rate reaction models for fracture in solids is given in ref. [4]; this comparison indicates that the models based on bond breaking rather than on bond slipping[6] are consistent with experimental results obtained on fracture in polymers and polycrystalline metals. However, in these models of fracture the growth of a single fatigue crack is not considered, which is of engineering interest.

Our approach will be different from those in refs [1–3] in that the growth of a single crack is of major importance, i.e. we are concerned with a cumulative damage process in which there is an observable.

3. DERIVATION OF A DAMAGE ACCUMULATION MODEL

We take the simplest approach in this initial study. To fix ideas, let us consider a thin center-crack panel under axial tension. Let w denote the thickness of the panel, l_0 the half-width, and $F(t)$ the axial tensile force.

Consider the cross-section of the panel formed by a plane perpendicular to the axis of the panel containing the crack which we assume lies in this cross-section. Let a denote the half mean crack length.† The panel is assumed thin so that we can assume the crack tip is straight and perpendicular to the panel face. Let ξ denote the distance along the axis of the cross-section from the centerline

†When we speak of crack length we always mean "mean" crack length from a distribution at time t even when this is not explicitly stated.

to a generic point in the portion of the cross-section ahead of the crack tip, i.e. $a \leqslant \xi \leqslant l_0$ (see Fig. 1). We observe that WOL geometry is the same as one-half a center crack panel, although stress distributions are different.

Let v denote the average number of atomic/nuclear bonds per unit cross-section area. Then

$$vw\,\mathrm{d}\xi = \text{average number of such bonds in the interval } (\xi, \xi + \mathrm{d}\xi) \text{ in the unbroken portion.}$$

If we assume that no appreciable bond breaking occurs ahead of the crack tip, it follows that

$$\int_a^{l_0} 2vw\,\mathrm{d}\xi = \text{total average number of unbroken bonds in the unbroken portion of the cross-section} = 2vw(l_0 - a). \tag{2}$$

This is an important step because it connects the macro variable crack length a with the micro bond breaking process. Since a is the only quantity that changes with time, eq. (2) implies that bond breaking is concentrated in the region of the crack tip.

Let $s(t, \xi)$ denote the normal stress at the point ξ in the unbroken cross-section at time t. We assume $s(t, \xi) = s(t, -\xi)$ and that this stress does not vary across the cross-section. We note that $s(t, \xi)$ is an average macro concept[18].

The normal force acting on the interval $(\xi, \xi + \mathrm{d}\xi)$ is

$$ws(t, \xi)\,\mathrm{d}\xi.$$

If we divide this average force by the mean numbers of bonds, $wv\,\mathrm{d}\xi$, in this interval, we obtain an approximation for the force f acting on a bond at ξ:

$$f = \frac{s(t, \xi)}{v}. \tag{3}$$

We now replace eq. (1) by

$$\kappa_b(t, \xi) = \frac{kT}{h}\,\mathrm{e}^{-\frac{\Delta G^* - \lambda s(t, \xi)/v}{kT}}, \tag{4}$$

or, with

$$\alpha = \frac{kT}{h}\,\mathrm{e}^{-\frac{\Delta G^+}{kT}}, \quad \beta = \frac{\lambda}{vkT}, \tag{5}$$

$$\kappa_b(t, \xi) = \alpha\,\mathrm{e}^{\beta s(t, \xi)}, \tag{6}$$

which is the mean rate of single bond breaking at point ξ at time t.

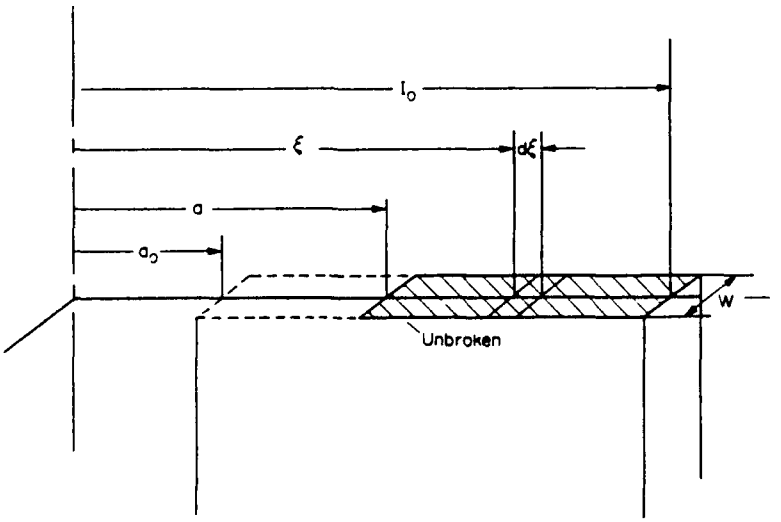

Fig. 1. Geometry of one-half of a center crack panel with some notation.

The macro average rate of bond breaking on the unbroken portion of the cross-section is thus

$$2\int_a^{l_0} w\nu\kappa_b \, d\xi = 2w\nu \int_a^{l_0} \alpha \, e^{\beta s(t,\xi)} \, d\xi. \tag{7}$$

Let us set this equal to the negative derivative with respect to time of the total average number of bonds, $2\nu w(l_0 - a)$, in the unbroken portion of the cross-section, obtaining

$$\frac{da}{dt} = \int_a^{l_0} \alpha \, e^{\beta s(t,\xi)} \, d\xi. \tag{8}$$

Neglecting dynamical effects, we have from equilibrium at time t,

$$F(t) = 2w \int_a^{l_0} s(t, \xi) \, d\xi. \tag{9}$$

We note that in eqs (8) and (9) $s(t, \xi)$ occurs under an integral sign with respect to ξ. This means that the right hand sides of eqs (8) and (9) will not be overly sensitive to how $s(t, \xi)$ depends on ξ, since $s(t, \xi)$ is a bounded function. Further, we note that eq. (8) is not of the form usually encountered in fracture mechanics; it is new and has been derived from physical theory. Since eqs (8) and (9) are basic in what follows, it is important at this point to make some comments on their derivation.

Simply put, to produce eq. (8) we evaluate the mean number of unbroken bonds at time t based only on geometry (see eq. 2) and equate the negative derivative with respect to time of this number to an expression for the mean rate at which bonds are being broken, as determined by the kinetic theory of thermally activated fracture (see eq. 7). The time dependent quantity in eq. (2) is the crack length $a(t)$; thus damage accumulation in this expression is measured by the macro quantity $a(t)$, with rate of accumulation proportional to $\dot{a}(t)$. On the other hand, the rate of damage accumulation according to eq. (7) depends on $s(t, \xi)$ as well as on $a(t)$. $s(t, \xi)$ not only depends on $a(t)$ but also on other quantities such as plastic zone size, for example. We note that eq. (8) can allow the possibility that additional macro observables may be present.

As stated, eq. (9) is an equilibrium result. This means that we assume the frequency content of $F(t)$ is well below the lowest natural frequency of the specimen that can be excited by axial loading. However, if dynamical results must be included, $s(t, \xi)$ will be related to $F(t)$ by a more complex relation than that given by eq. (9).

We have approximated f (see eq. 3) by means of the average macro quantity $s(t, \xi)$. Thus, we are employing a smoothed version of f. However, in a real material, f as well as λ will change from bond to bond due to variability in material properties as noted by Zhurkov[3]. It follows that when such variability is to be taken into account, we must re-examine our evaluation of λf.

α and β contain the temperature T. In the constant stress tests of Zhurkov[3], the temperature was held constant. However, T may increase when $F(t)$ is cyclic, as is well known when the frequency is high. Hence, T may be time dependent.

Next, β contains the material parameter λ. Zhurkov[3] as well as others[1, 2] assumed λ was a constant in time to failure under static tests, and this was not contradicted by the experimental results. However, where damage accumulation is being studied under cyclic load, this may not be the case.

Finally, we observe that eqs (8) and (9) apply to a particular geometry, i.e. to either a center crack panel or to a WOL specimen. Other geometries of crack development will require a different formulation. Such possibilities will not be considered in this initial study.

4. SOME SIMPLE MACRO-MODELS OF DAMAGE ACCUMULATION

At this initial stage in our investigation of what can be learned from eqs (8) and (9), it is appropriate to confine attention to simple situations. To that end, let us first assume

$$s(t, \xi) = s(t), \tag{10}$$

which means that the stress is uniform over the unbroken portion of the panel cross-section. We first find from eq. (9)

$$s(t) = \frac{F(t)}{2w(l_0 - a)}. \tag{11}$$

From eq. (8), we then obtain

$$\frac{da}{dt} = \alpha \int_a^{l_0} e^{\beta s(t)}\, d\xi = \alpha(l_0 - a)\, e^{\beta s(t)} \tag{12}$$

or

$$\frac{da}{dt} = \alpha(l_0 - a)\, e^{\frac{\beta F(t)}{2w(l_0 - a)}}. \tag{13}$$

The substitutions

$$y = \frac{a}{l_0}, \quad \frac{F(t)}{2wl_0} = s_0(t), \tag{14}$$

where $s_0(t)$ is the far field axial stress, change eq. (13) to

$$\frac{dy}{dt} = \alpha(1 - y)\, e^{\frac{\beta s_0(t)}{1 - y}}. \tag{15}$$

Different forms of this equation appear in refs [2, 4], where it is assumed $s_0(t) =$ constant, i.e. the constant load case. When the load or stress is constant, eq. (15) can be integrated to yield a time to failure expression[2], and it is this expression that not only provides an excellent description of the time to failure data due to Zhurkov[3] at different constant loads and different temperatures, but it also provides an accurate predictor of time to failure where the load and/or temperature are changed from the values at which α and β are initially estimated.

Zhurkov actually does not start from eq. (15). Rather he employs a time to failure expression obtained by fitting an exponential formula to the extensive data that he collected. The empirical expression he obtained can be obtained from the integrated form of eq. (15) by using suitable approximations. For a discussion of this point, see ref. [5].

In refs [6, 7], $s(t)$ is assumed simple harmonic about a mean value (>0). Equation (8) is then numerically integrated, and the results compare well, in the example considered, with the single specimen test result. In ref. [7], they also consider this case employing a different method.

Equation (15) is the simplest form we can obtain from eqs (8) and (9). It has one observable or measure of damage accumulation, namely y. However, an objection to eq. (15) can be raised. It stems from the fact that the stress is assumed uniform, i.e. independent of ξ, which means there is no physical reason why there cannot be significant bond breaking well ahead of the crack tip although we assumed in eq. (2) the contrary. To partially overcome this objection let us next assume.

$$s(t, \xi) = s(\xi)g(t), \tag{16}$$

where the stress factor $s(\xi)$ only depends on ξ and $g(t)$ is a multiplicative time factor. In view of the fact that the normal stress is high in the irreversible bond breaking region and then decreases to an elastic stress as we move away from the crack tip, a more realistic assumption for $s(\xi)$ is either

$$\begin{aligned} s(\xi) &= \sigma_p, && a \leqslant \xi \leqslant a + \Delta, \\ &= \sigma_e (< \sigma_p), && a + \Delta < \xi \leqslant l_0, \end{aligned} \tag{17a}$$

or

$$\begin{aligned} s(\xi) &= \sigma_p + \frac{\Delta + 2a}{\Delta}\Delta\sigma - \frac{2\Delta\sigma}{\Delta}\xi, && a \leqslant \xi \leqslant a + \Delta, \\ &= \sigma_e, && a + \Delta < \xi \leqslant l_0, \end{aligned} \tag{17b}$$

where $\Delta < l_0 - a$ and $0 < \Delta\sigma < \sigma_p - \sigma_e$. Equation (17a) gives two constant stress regions as does the second region in eq. (17b). However, in the region $a \leqslant \xi \leqslant a + \Delta$, eq. (17b) permits the stress

to vary linearly from $\sigma_p + \Delta\sigma$ to $\sigma_p - \Delta\sigma > \sigma_e$ with mean value σ_p. Thus, in eq. (17b), the stress at the crack tip is the largest in the unbroken cross-section, which means that the maximum rate of bond breaking occurs at the crack tip even if $\Delta\sigma$ is small. If $\Delta\sigma = 0$, eqs (17a) and (17b) are the same.

We find from eq. (9), using either eq. (17a) or (17b), that the dimensionless time factor is

$$g(t) = \frac{s_0(t)/\sigma_e}{(1 - y - \delta + r_\sigma \delta)}, \tag{18}$$

where $\delta = \Delta/l_0$, $\sigma_p/\sigma_e = r_\sigma = 1 + \epsilon$, and, as before, $s_0(t) = F(t)/2wl_0$ is the far field stress. The substitution of eqs (18) and (17a) into eq. (8) produces

$$\frac{dy}{dt} = \alpha[\delta\, e^{\frac{\beta r_\sigma s_0(t)}{1 - y - \delta + r_\sigma \delta}} + (1 - y - \delta)\, e^{\frac{\beta s_0(t)}{1 - y - \delta + r_\sigma \delta}}]; \tag{19a}$$

if eq. (17b) is employed, eq. (19a) is replaced by

$$\frac{dy}{dt} = \alpha\delta\, e^{\frac{\beta r_\sigma s_0(t)}{1 - y - \delta + \sigma_0 \delta}} \frac{\sinh\left(\frac{\beta s_0(t)\Delta\sigma'}{1 - y - \delta + r_\sigma \delta}\right)}{\left(\frac{\beta s_0(t)\Delta\sigma'}{1 - y - \delta + r_\sigma \delta}\right)}$$

$$+ \alpha(1 - y - \delta + r_\sigma \delta)\, e^{\frac{\beta s_0(t)}{1 - y - \delta + r_\sigma \delta}}, \tag{19b}$$

where $\Delta\sigma' = \Delta\sigma/\sigma_e$. If $\delta = 0$, both reduce to (15).

Equation (19b) is approximately equal to eq. (19a) for $\Delta\sigma' \ll 1$. Hence, we shall use eq. (19a) in subsequent work since it is the simpler of the two from the parameter estimation point of view, and we do not have to consider $\Delta\sigma'$.

We note that in eq. (19a) there are three observables or measures of damage accumulation, namely, y, δ and r_σ or ϵ. We must either obtain expressions for the joint evolution of y, δ and ϵ, or we must assume that δ and ϵ depend on y in some explicit manner if y is the only one observable. We shall see, after confronting data, that for these data the major portion of atomic bond breaking does not occur in the region $a + \Delta < \xi \leqslant l_0$ if $\epsilon > 0.20$.

5. APPLICATION OF EQS (15) AND (19) EXPERIMENTAL DATA ON MEAN CRACK GROWTH

The purpose of this section is to confront the model defined by eqs (15) and (19) with data. We shall consider four sets of data on FCG under simple harmonically varying tensile load:

(a) ASTM E24.04.01 round robin data, 10Ni–8Co–1Mo steel, 24 replications[8].
(b) Virkler, Hillberry, Goel (VHG) data, 2024-T3 aluminum, 68 replications[9, 10].
(c) Ichikawa, Hamaguchi, Nakamura (IHN) data, 2024-T3 aluminum, 30 replications[11].
(d) Ghonem, Dore (GD) data, 7075-T6 aluminum, 60 replications[10, 12].

Equations (15) and (19) refer to mean crack length a or its dimensionless version y. For parameter estimation, we require an estimate of how a or y varies with cycle number or time. Mean crack length is obtained by averaging over the a-values of the sample functions (of a vs time) at a fixed time. Available data analysis[10] is for mean time to reach a given crack length that is obtained by averaging over the time-values of the sample functions at a fixed crack length. In either case a y vs t curve is obtained in which the term "mean" is applied to only y or to t. Examination of the VHG data presented in ref. [10] reveals that the two curves are close to one another (see Appendix). Thus, for the y vs t curve, we shall use the mean time vs y curve which is sufficiently close to the mean y vs t curve for our purposes.

Equations (15) and (19) contain the two physical parameters

$$\alpha = \frac{kT}{h} e^{-\frac{\Delta G^*}{kT}}, \quad \beta = \frac{\dot{\lambda}}{\nu k T}. \tag{20}$$

ΔG^+ can be estimated in one of two ways. Zhurkov has estimated ΔG^+ from simple tests on time to failure under static load, however, Zhurkov[3] has also shown that ΔG^+ can be obtained from the heat of sublimation in metals[13]: thus, there are two methods for estimating ΔG^+, and, hence for estimating α. β cannot be estimated from existing physical data since it depends on the test conditions plus the manufacturing process. It follows that β must be estimated from test data. We note that Zhurkov's simple tests for estimating β under static load may give values that do not apply with cyclic loads.

The data in the four cases consist of a vs n (cycles) from which we obtain the values of Δt_j corresponding to Δa_j or Δy_j. We shall use $(\Delta t_j, \Delta y_j)$ to estimate β in eq. (15) for the first data set and in eq. (19) for all four data sets. There are several reasons for doing this: firstly, it is important to determine whether or not β depends on $y = a/l_0$ or time t; secondly, if β depends on these quantities, it is important to determine if that dependence can say something about the FCG process and its modeling; finally, it is important to determine what must be known in order to make accurate predictions.

(*a*) *ASTM E*24.04.01 *round robin data*[10]

The material is 10Ni–8Co–1Mo steel. The WOL-type test specimens 0.250 in. thick were cut from the same sheet of material. The load employed is

$$F(t) = 605 + 495 \sin \omega t \text{ (lb.)}, \tag{21}$$

where $\omega = 10\,\pi$/s. Tests were conducted at different laboratories. From the results obtained, we selected 24 specimens as usable for our statistical analysis[14]. A load shedding program was employed to produce the initial crack length, which differed among the laboratories. It is appropriate, therefore, to take the initial crack length, $a_0 = 1.0$ in. With $\Delta a = 0.05$ in. and $l_0 = 2.55$ in. The (t, a) data are available at 20 points for purposes of parameter estimation.

The material is steel. If we regard the material to be iron, then according to ref. [15] $\Delta G^+ = 94{,}000$ cal/mol. We take $T = 300$ K as a representative temperature, and find

$$\alpha = 1.9655 \times 10^{-56}/\text{s}. \tag{22}$$

The parameter β_j must be estimated from the $(\Delta t_j, \Delta y_j)$ data.

Let us approximate eq. (15) by the difference form

$$\Delta y_j = \alpha(1 - \bar{y}_j)\,\Delta t_j \frac{1}{2\pi} \int_0^{2\pi} e^{\frac{\beta_j \bar{s}_0}{1-\bar{y}_j}(1 + \Delta s' \sin \tau)}\, d\tau \tag{23}$$

where

$\Delta y_i = \Delta a_j / l_0$ (jth y-increment),

$\bar{y}_j = \dfrac{a_j + a_{j+1}}{2l_0}$ (mid value for y_j, y_{j+1}),

$\Delta t_j =$ times increase of y_j by Δy_j,

$\beta_j = \dfrac{\lambda_j}{vkT}$ or $\beta_y = \dfrac{\lambda_y}{vkT}$,

$\bar{s}_0 =$ constant far field mean stress,

$\Delta s =$ time varying far field stress amplitude,

$\Delta s' = \Delta s / \bar{s}_0$, and

$\tau = \omega t$.

For this initial study, we will make the computational simplifications of replacing the sine wave form by a rectangular wave form:

$$\frac{2}{\pi} \quad \text{for } 0 < \tau \leqslant \pi,$$

$$-\frac{2}{\pi} \quad \text{for } \pi < \tau \leqslant 2\pi. \tag{24}$$

Then

$$\frac{1}{2\pi}\int_0^{2\pi} e^{\frac{\beta_j \bar{s}_0}{1-\bar{y}_j}(1+\Delta s' \sin\tau)}\,d\tau \simeq \frac{1}{2} e^{\frac{\beta_j \bar{s}_0}{1-\bar{y}_j}}, \tag{25}$$

where

$$\bar{s}' = \bar{s}_0\left(1 + \frac{2\Delta s'}{\pi}\right) \tag{26}$$

and where the term arising from the second part of eq. (24) is neglected since in the data analysis it will be found that this term is very small relative to the contribution from the first part of eq. (24). Equation (23) is thus replaced by

$$\Delta y_j = \frac{\alpha}{2}(1-\bar{y}_j)\,\Delta t_j\, e^{\frac{\beta_j \bar{s}_0}{1-\bar{y}_j}}. \tag{27}$$

Since Δy_j, α, $\bar{y}_j$ and Δt_j, are known, we can estimate $\beta_j \bar{s}_0$ from this equation.

Figure 2 shows the $\beta_j \bar{s}_0'$ estimates as a function of $\bar{y}_j$ (or $\bar{a}_j$) and t_j. When the estimates are plotted against t_j (Fig. 2a) a decreasing nonlinear function is obtained. On the other hand, when they are plotted against $\bar{y}_j$ (Fig. 2b, top line), the straight line character of these estimates is remarkable. Since it is easier to work with a straight line than a nonlinear function, we prefer the latter. The least square linear fit to these estimates is

$$\beta_y \bar{s}_0' = 116.921(1 - 0.98788y), \tag{28}$$

where $\beta_y \bar{s}_0'$ is dimensionless. Before discussing some of the implications of this result, let us use the form in eq. (19a).

Equation (19a) contains the two additional parameters r_σ and δ. Let us replace r_σ by $1+\epsilon$. We know the plastic region increases in length as the crack grows. In this initial study, we make the simple assumption that $\delta = zy$, $0 \leqslant z < 1$, recognizing that this is an assumption of importance and it will be discussed below. Thus, we introduce the constraint

$$r_\sigma = 1 + \epsilon, \quad \delta = zy, \tag{29}$$

where ϵ and z constant. We follow the same procedure as we employed in obtaining (27) to find from (19a)

$$\Delta y_j = \frac{\alpha}{2} z\bar{y}_j\,\Delta t_j\, e^{\frac{\beta_j(1+\epsilon)\bar{s}_0}{1-(1-\epsilon z)y}} + \frac{\alpha}{2}[1-(1+z)\bar{y}_j]\,\Delta t_j\, e^{\frac{\beta_j \bar{s}_0}{1-(1-\epsilon z)\bar{y}_j}}. \tag{30}$$

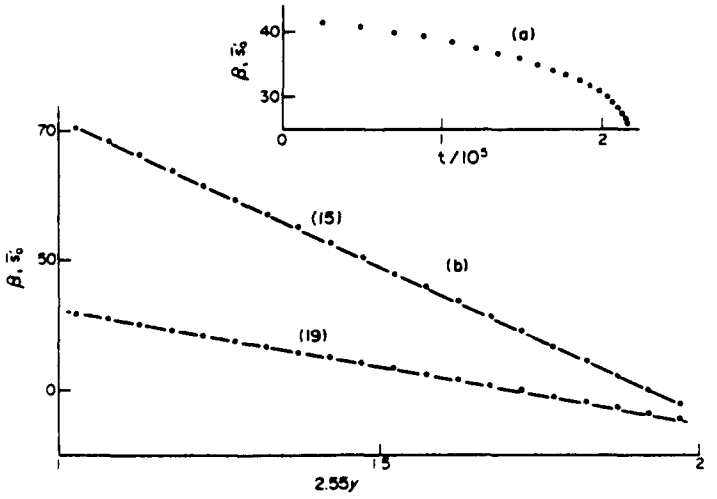

Fig. 2. (a) $\beta_j \bar{s}_0'$ estimate from the ASTM data plotted against time t_j; (b) $\beta_j \bar{s}_0'$ estimates plotted against y_j based on eqs (15) and (19). $\Delta y_j = 0.05/2.55$.

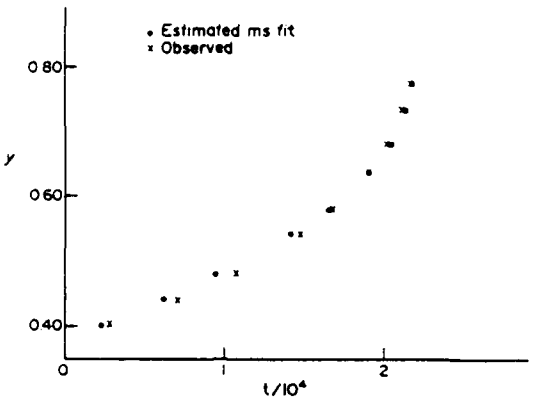

Fig. 3. Comparison of estimated and observed y vs t points for ASTM data, where estimated curve employs eq. (27) and uses $\beta_j \bar{s}_0'$ from eq. (32) rather than data.

Let us take $\epsilon = 1$ and $z = 0.25$ as representative for our present purposes. We quickly find on confronting the data that the second term is orders of magnitude smaller than the first term on the right hand side of eq. (30). Hence, eq. (30) becomes in practice

$$\Delta y_j = 0.125\alpha \bar{y}_j \Delta t_j e^{\frac{2\beta_j \bar{R}_0}{1 - 0.75\bar{y}_j}}. \tag{31}$$

Figure 2(b) (see lower line) also shows the estimates $\beta_j \bar{s}_0'$ vs $\bar{y}_j$†. The straight line character of these estimates still obtains. The least squares estimate of this line obtained from the estimates is

$$\beta_y \bar{s}_0' = 59.2759\ (1 - 0.73625y). \tag{32}$$

Thus, regardless of whether we use eqs (15) or (19a) the $\beta_j \bar{s}_0'$ estimates vs $\bar{y}_j$ can be accurately approximated by a straight line. What does this result say?

Consider $\beta \bar{s}_0' = (\lambda \bar{s}_0'/vkT) \cdot \bar{s}_0'$ is a constant as are v, k and by assumption T. Thus, if $\beta \bar{s}_0'$ decreases with y, this means that λ decreases with y also. λ determines the strength of the material, where, as discussed in connection with eq. (1), when λ is high means that the material is weaker than when λ is low. Figure 2 shows that λ is decreasing linearly with y; this means the material (just ahead of the crack tip) is getting stronger as the crack length increases; this, in turn, means that, since there is no external source acting to produce a material change, the material is work hardening at a constant rate as y increases. What we learn from this model is that the rate at which work hardening is taking place is constant as a function of y, and this is a new way to demonstrate that fact. The same results hold whether we use eq. (15) or (19a) which is also remarkable.

Further comments will be delayed until remaining data sets are examined.

Figure 3 plots the mean crack growth curve as observed and one predicted from (27) with $\beta_j \bar{s}_0'$ estimated from (32) rather than from the data. The agreement is all one could expect.

(b) VHG data[9, 10, 14]

The material is 2024-T3 aluminum alloy. The specimen is a center crack panel 558.8 mm long with a half-width $l_0 = 76.2$ mm and thickness of 2.54 mm. The load is

$$F(t) = 3150 + 2110 \sin \omega t \text{ (lb.)} \tag{33}$$

with $\omega = 40\pi$ rad/s, 68 replications were used. Data were recorded as cycles to reach a given crack length. A load shedding program was employed to produce the initial crack of $a_0 = 9$ mm; the maximum crack length employed was 49.8 mm. Three crack length intervals Δa were employed, namely, 0.2 mm, 0.4 mm and 0.8 mm, $l_0 = 76.2$ mm and (t, a) is available at different numbers of points.

†Here we use $\Delta G^* = 93{,}040$ cal/mol which takes into account the fact that the material is not *all* iron. This gives $\tau = 1.94547 \times 10^{-16}$ s.

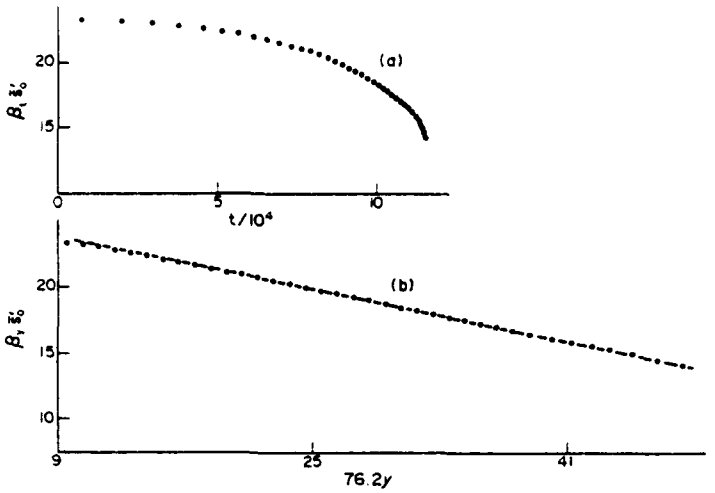

Fig. 4. (a) $\beta_i \bar{s}_0'$ estimates from VHG data plotted against time t_j. (b) $\beta_i \bar{s}_0'$ estimates plotted against y_j. $\Delta y_j = 1/76.2$.

The data analysis in refs [10, 14] estimated the mean time to reach a specified crack length. As mentioned earlier, we shall use these available data to estimate mean crack length at a specified time since the difference is small between the two cases.

Zhurkov[3] found from experimental data that $\Delta G^+ = 53{,}000$ cal/mol for polycrystalline aluminum, whereas [14] gives 55,000 cal/mol for aluminum; we shall use Zhurkov's value which gives, with $T = 300$ K,†

$$\alpha = 1.4878 \times 10^{-26}/\text{s}. \tag{34}$$

We shall only use eq. (19a) from this point on since it is in better agreement with the facts on stress distribution than eq. (15).

We again use $\epsilon = 1$, $z = 0.25$ which means we use eq. (31). Figure 4(a) shows the $\beta_j \bar{s}_0'$ estimates plotted against time t, and Fig. 4(b) plots the same estimates vs y. These graphs are similar in form to those shown in Fig. 2 for steel. The first figure indicates that λ is decreasing in a nonlinear manner with time; i.e. work hardening is a nonlinear increasing function of time. Figure 4(b) again shows that, except in the initial portion, the $\beta_j \bar{s}_0'$ estimates are remarkably close to a straight line. Let us examine this initial portion in greater detail.

The $\Delta a_j = 1$ mm (or $\Delta y_j = 1/76.2$) in the initial portion of Fig. 4(b). Let us use now $\Delta a = 0.20$ mm. The results are plotted in Fig. 5(a) for $9 \leqslant a \leqslant 13.2$ mm. It is clear that there is a departure from a straight line in this interval. On the other hand, if we examine the interval $15 \leqslant a \leqslant 17.2$ mm, with $\Delta a = 0.20$ mm, we obtain the results shown in Fig. 5(b) where the straight line approximation is excellent. We did not encounter this departure from a straight line in the initial portion of Fig. 2 for steel. What might cause this departure from a straight line?

It is our opinion that in the interval $9 \leqslant a \leqslant 15$ mm the effect of the load shedding program is still present. The reason we did not see this feature in Fig. 2 is that the data considered started at $a_0 = 1.0$ in. which may have eliminated the effect of the load shedding program that might have been present if we used an $a_0 < 1.0$ in. The interesting point to observe is that we now have a method for detecting when the effect of load shedding ceases.

We see from Fig. 4(b) that if we start at 15 mm, the $\beta_j \bar{s}_0$ estimated when plotted against y_j are essentially on a straight line. The least squares estimate for this line is

$$\beta_j \bar{s}_0' = 26.20280\ (1 - 0.72878y). \tag{35}$$

(*c*) *IHN data*[16]

The material is 2024-T3 aluminum alloy. The specimen is a center crack panel 400 mm long, 70 mm wide, and 1 mm thick. The load is

$$F(t) = 706 + 468 \sin \omega t \text{ (lbs)} \tag{36}$$

†Actually $T = 307$ K but this is sufficiently close to 300 K for our purposes.

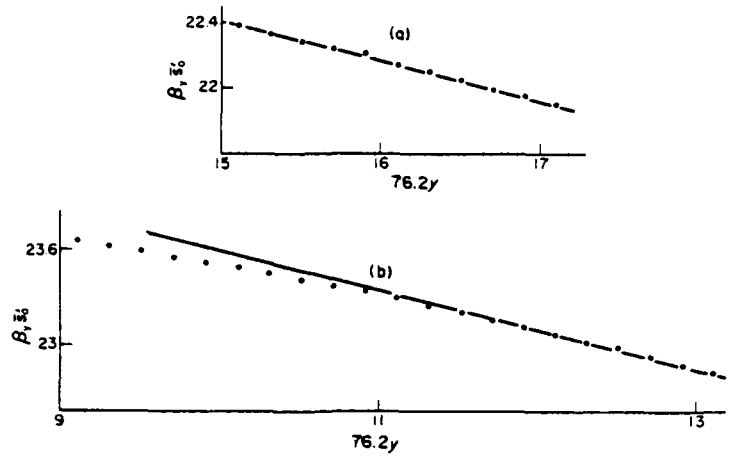

Fig. 5. $\beta_j \bar{s}_0'$ estimates from VHG data plotted against y_j. $\Delta y_j = 0.20/76.2$. Two y-intervals are shown.

with $\omega = 36.8\,\pi$ rad/s, 30 replications were used. Data were recorded as crack length to reach a given number of cycles. A load shedding program was employed to produce the initial average crack length of $\bar{a}_0 = 7.0302$ mm, $l_0 = 35$ mm. T is assumed to be 300 K, and we use α from eq. (34). The (t, y) data are available at 8 points for purposes of parameter estimation.

The data analysis[10] estimated the mean time to reach a specified crack length which we use as in the above. We use (19a) with $\epsilon = 1$ and $z = 0.25$. After the first point, $\Delta y_j = 2/35$.

Figure 6 plots the $\beta_j \bar{s}_0'$ estimates vs $\bar{y}_j$. After the first point, the estimates lie on a straight line with excellent accuracy. The least square estimate of the line is

$$\beta_y \bar{s}_0' = 26.124396(1 - 0.72293y) \tag{37}$$

where the first point is ignored. The first point does not lie on the line due to the effect of the load shedding program.

The material in these data and the Virkler data is 2024-T3 aluminum alloy. However, the specimen thicknesses are 1 mm and 2.54 mm, respectively. This means that the material preparations are different. Thus, the parameters in eq. (37) will be different from those in eq. (35).

(d) GD data

The material is aluminum 7075-T6 alloy. The specimen is a center crack panel 320.67 mm long, 101.6 mm wide, and 3.175 mm thick; thus $l_0 = 50.8$ mm. Three load conditions are involved:

$$\begin{aligned} &\text{Test \# 1}, \quad F(t) = 4099 + 1024 \sin \omega t \text{ (lb.)}, \\ &\text{Test \# 2}, \quad F(t) = 3752 + 1250 \sin \omega t \text{ (lb.)}, \\ &\text{Test \# 3}, \quad F(t) = 2391 + 1024 \sin \omega t \text{ (lb.)}, \end{aligned} \tag{38}$$

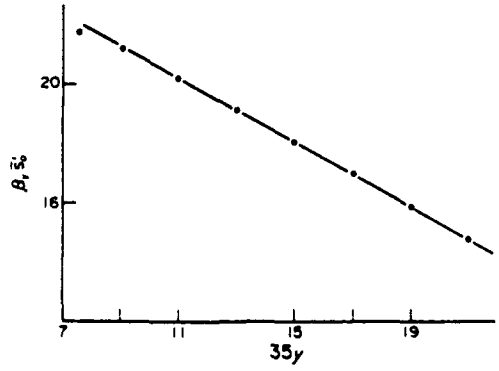

Fig. 6. $\beta_j \bar{s}_0'$ estimates plotted against y_j for the IHN data. $\Delta y_j = 2/35$ after first interval.

with $\omega = 20\,\pi$ rad/s, 60 replications were used in each test. A load shedding program was employed to produce an initial crack length $a_0 = 9$ mm. The (t, y) data are available at 6 points for purposes of parameter estimation.

These available data analysis uses three Δy_j:

$$\begin{aligned} &\text{Test\#1,} \quad \Delta y_j = 0.0360827, \\ &\text{Test\#2,} \quad \Delta y_j = 0.0393708, \\ &\text{Test\#3,} \quad \Delta y_j = 0.0328150. \end{aligned} \tag{39}$$

The data analysis estimates the mean time to reach 6 crack lengths starting at $a_0 = 9$ mm. With $T = 300$ K,

$$\alpha = 1.4878 \times 10^{-26}/\text{s}$$

as in the case for data sets (b) and (c). Again we use $\epsilon = 1$, $z = 0.25$, which thus makes eq. (31) applicable. Figure 7(a) shows the $\beta_j \bar{s}_0'$ estimates plotted against y as abscissa for each of the three test conditions. Except for the first point, the remainder can be accurately approximated by a straight line for each condition. A few comments are in order.

First, the residual effect of the load shedding program explains why the first point is below the straight line for each condition; the same residual effect was noted for the data sets (b) and (c).

While it is no longer remarkable to obtain these straight lines, it is remarkable that the three lines are almost parallel. The least square fit of a straight line to these estimates, excluding the first point, is

$$\begin{aligned} &\text{Test\#1:} \quad \beta_y \bar{s}_0' = \beta_0 \bar{s}_0'(1 - 0.71978y), \quad \beta_0 \bar{s}_0' = 25.9862, \\ &\text{Test\#2:} \quad \beta_y \bar{s}_0' = \beta_0 \bar{s}_0'(1 - 0.72546y), \quad \beta_0 \bar{s}_0' = 26.1707, \\ &\text{Test\#3:} \quad \beta_y \bar{s}_0' = \beta_0 \bar{s}_0'(1 - 0.71895y), \quad \beta_0 \bar{s}_0' = 25.6854, \end{aligned} \tag{40}$$

the slopes being respectively -18.7044, -18.9858, -18.4665. These slopes are slightly different but the differences will not show up on a graph. We also note that the coefficient of y in the parentheses are very close in value in the three cases; the average is 0.72140 with a maximum difference of 0.56%. In view of the fact that the currently available data analysis only provides 5 points with which to estimate each line, these numerical values cannot be viewed as final although they are interesting.

Third, we know $\bar{s}_{0,k}'$ in each case; thus we find

$$\begin{aligned} &\text{Test\#1:} \quad \bar{s}_{0,1}' = 9560 \text{ psi}, \quad \beta_{0,1} = 0.002718/\text{psi}, \\ &\text{Test\#2:} \quad \bar{s}_{0,2}' = 9150 \text{ psi}, \quad \beta_{0,2} = 0.002860/\text{psi}, \\ &\text{Test\#3:} \quad \bar{s}_{0,3}' = 6120 \text{ psi}, \quad \beta_{0,3} = 0.004197/\text{ psi}. \end{aligned} \tag{41}$$

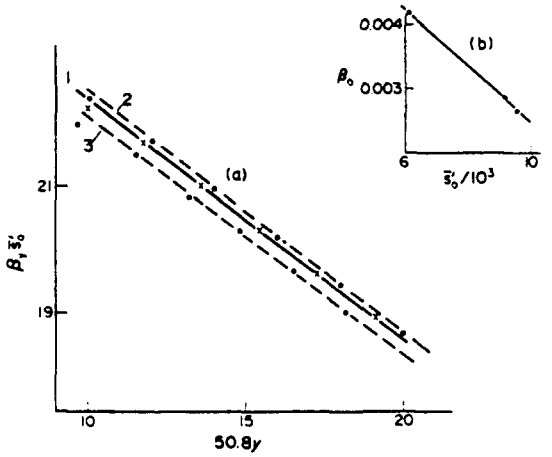

Fig. 7. (a) $\beta_j \bar{s}_0'$ estimates plotted against y_j for the these load conditions of the GD data. Δy_j variable; (b) β_0 estimates plotted against $\bar{s}_0'$ for these load conditions.

The $\beta_{0,k}$ estimates are plotted against $\bar{s}_0'$ in Fig. 7(b). We note these estimates lie close to a straight line, although the points are not well spaced. The least square linear fit obtained from eq. (41) is

$$\beta_0 = 0.006838 - 4.32535 \times 10^{-7}\bar{s}_0'. \tag{42}$$

Thus, (42) suggest that given any $\bar{s}_0'$ we can calculate β_0 for this $\bar{s}_0'$. Since all coefficients of y in (39) are close to 0.72140, this further suggests that prediction of mean crack growth at $\bar{s}_0'$ different from those tested might be possible. More will be said about this below.

Finally, we observe in eq. (41) that the β_0 are different for different $\bar{s}_0'$. Since

$$\beta_0 = \frac{\lambda_0}{\nu k T}, \tag{43}$$

the results in eq. (41) say that λ_0 depends on the loading through $\bar{s}_0'$.This means that the work hardening process depends on the loading as well as on the dimensionless crack length y as indicated by eq. (40). We thus see that $\beta_y \bar{s}_0'$ depends on the two fixed material parameters β_0 or λ_0 and the coefficient of y in eq. (40), of which β_0 depends strongly on the loading through $\bar{s}_0'$ whereas the coefficient of y does not seem to do so.

The GD data are the most interesting of the four sets (a), (b), (c) and (d) considered in this section, because of the three sets of loads employed. However, a data analysis with more than 15 points in each of the three crack length intervals is needed to improve the accuracy of the values given in eqs (40) and (41).

Let us next discuss what can be said when the four data sets are considered together.

6. DISCUSSION

The consistency of the character of the estimates of $\beta_y \bar{s}_0'$ from four data sets involving different metals, load means and amplitudes, and laboratories is certainly remarkable. We have already discussed in the previous section some of the physical inferences that can be drawn from these consistent results on mean behavior in metals where geometry of the crack development is essentially the same. There are many points that merit further discussion. However, in this initial paper, we only can take up a few.

Equations (8) and (9) are the starting point for this study at the macro or engineering level. Equation (9) is a force balance equation and requires no further comment here. Equation (8) says that two ways of evaluating the macro mean rate of bond breaking are equal, and relates $\dot{a}(t)$ to the bond breaking process in the unbroken portion of the cross-section. It is important to realize that the left-hand side of eq. (8) implies that all the bond breaking takes place at the crack tip or at least in a small region just ahead of the crack tip. Obviously, the right hand side must say the same thing.

We approximated f in eq. (3) by means of the normal stress $s(t, \xi)$. Stress is an average concept. Love[16] has pointed out that it is a "macroscopic or large-scale" concept, which means we are using a smooth version of f. While this is the simplest method of approximating f for the geometry and loading under consideration, it may not be the only possibility that merits attention[17]. Further, with different specimens geometry and method of applying the load, the normal stress $s(t, \xi)$ will not be appropriate, and we leave this point to another time. Let us next focus attention on the normal stress.

The choice of $s(t, \xi)$ in eqs (8) and (9) is basic to what follows. As noted earlier, $s(t, \xi)$ always occurs under an integral sign with respect to ξ, and this means that the broad features of its form as a function of ξ are important but not the details. When a macro crack is present, a uniform normal stress is not realistic. Equation (17) does contain the broad features that $s(t, \xi)$ must possess, and this is the simplest choice that can be made possessing these features (see ref [18] for a different approach). However, this choice requires the addition of the two new quantities Δ or δ and r_p when eq. (17a) is employed. At this time, there are no experimental data to suggest how these two quantities behave. Qualitatively, we know that the plastic zone increases in length and work hardening increases as time or crack length increases for the materials considered. However, we have no quantitative information on how y, δ, and r_p jointly evolve with time or if they may be regarded as a state vector[10]. To circumvent this current lack of information and get on with a preliminary parameter estimation study, we assume the constraint eq. (29), which is at least

physically plausible. Clearly, it is important to obtain experimental data on how y, δ and r_n jointly evolve with time in order to refine and/or expand the scope of this model.

We employ the same $s(t, \xi)$ for center crack panel and WOL specimens under tensile loading. This choice can be questioned. However, we see from the data analysis with $\epsilon = 1$ and $z = 0.25$, that the high stress region produces the overwhelming fraction of bond breaking that takes place. This would still be the case if $\epsilon \geqslant 0.20$. Thus, the precise form of $s(t, \xi)$ in the low stress region, which will differ between the specimen types, is not important.

The crack growth process is more complex than failure under constant stress[3]. To see this, let us write

$$\beta_y \bar{s}_0' = \beta_0 \bar{s}_0'(1 - cy), \tag{44}$$

which conforms to all cases considered. The substitution of eq. (44) into the first term of eq. (30) gives

$$\Delta y_j = \frac{\alpha z}{2} \bar{y}_j \, \Delta t_j \, e^{\frac{\beta_0 \bar{s}_0'(1+c)(1-c\bar{y}_j)}{1-(1-c)\bar{y}_j}}, \tag{45}$$

which implies $\epsilon > 0.20$. Instead of the two constant material parameters α and β employed in refs [2, 3], we now have three, namely, α, β_0 and c. The parameter α depends on the material but not on the load; β_0 depends on the material and the load; and c depends on the material but not strongly on the load. Thus, the parameter estimation problem and the model defined by eq. (45), which uses eq. (29), is more complex than the models considered by previous investigators. This fact has been established with the aid of four high replication sets of FCG data.

The presence of T in an explicit manner, in α and β_0, is important. Its presence indicates that it should be measured during tests. Further, since relatively small changes in T can produce substantial changes in fatigue life, lack of knowledge of how T may be changing can introduce a source of life variability that may produce incomprehensible results as well as unwanted consequences. Thus, having T explicitly present, is a source of strength for the current model.

The purpose of the load shedding program in FCG tests is to eliminate the transient material behavior that is induced when the initial crack length is rapidly produced. Consider the upper graph in Fig. 5 which refers to the 15 to 17 mm crack length interval. The $\beta_j \bar{s}_0'$ estimates essentially lie on a straight line, indicating in our view, that the rate of work hardening is constant. We interpret this to mean material behavior has reached a steady state. The lower graph, which is for the 9 to 13 mm interval, shows an initial departure from steady state material behavior. We believe this effect is due to the lingering effect of the load shedding program. This appears to be the first model that can, from a data analysis, detect this lingering effect. Hence, this is a remarkable feature of the model. There is another point worthy of comment.

Consider the lower graph in Fig. 4, which is for the 9 to 49 mm crack length interval. The straight line character of the estimates persists to the largest a-values employed, where the crack tip is coming close to the panel edge. The same feature is observed in Figs 2, 6 and 7. It is reasonable to expect that the close proximity of the crack tip to the specimen edge would disturb the constant rate of work hardening in view of the fact that the lingering effect of load shedding does change the rate. Thus, it is a surprise that there is no change in the rate due to the edge effect, even in Fig. 2 where the crack tip comes to within 0.55 in. of the specimen edge.

Numerous approximations were made in obtaining eqs (27) and (31). For example, the varying y-value on a Δy_j interval was replaced by the constant $\bar{y}_j$; $\sin \tau$ was replaced by a square wave function; and because of the numerical values of the parameter being estimated and our choice $\epsilon = 1$, certain terms became negligible and were dropped. In a preliminary study, these approximations are acceptable. However, now that we have found that the model is interesting, it becomes necessary to refine our parameter estimation study by eliminating these approximations, and this will be done in a future study.

The model presented is for mean behavior. However, we mentioned earlier that if variability is to be included, we must re-examine our evaluation of the term λf, although this term may not be the only source of variability. What makes this term of interest is that f and λ vary from bond to bond due to variability in the atomic structure of the material. Further, due to the polycrystalline nature of the material, different crystals and grain boundaries will be stronger than others providing

possible correlation in λ-values over intervals of varying lengths. These possibilities are some that will be of interest when variability is taken into account, which we also leave to a future paper.

7. CONCLUSION

The model presented for mean fatigue crack growth is based on fundamental results provided by physical theory. The starting point for the derivation of the model is the basic expression for the mean rate of single atomic bond breaking provided by the kinetic theory of thermally activated bond fracture. Based on this expression, which applies at the micro level, a macro model is derived for mean fatigue crack growth, as a function of time, in a center crack panel and WOL test specimen under (simple harmonically varying) tensile load. The parameters in the model have physical meaning due to either the time varying load or material properties. In this paper, only the simplest version is considered.

The ideas employed here differ in a fundamental manner from those employed in fracture mechanics. In this paper, basic ideas from physics are brought in at the atomic level at the outset. This is different from the traditional approach and offers a basic approach that has not been previously studied. The model is not phenomenological.

The most significant point of the macro equations and parameter estimates that have been developed is their engineering importance. The most important feature for the engineer is that for a specific component only two or at most three tests are required to predict mean fatigue growth for an arbitrarily varying simple harmonic tensile load.

We see from eq. (45) that there are three parameters, namely, α, β_0 and c that must be estimated in order to use this equation for prediction of mean fatigue life behavior. The parameter α can be estimated from tabulated data. The parameters β_0 and c must be estimated from tests. While β_0 depends on $\bar{s}_0$ and Δs through $\bar{s}_0'$, c does not seem to depend on these quantities. We observe from the GD-data analysis that two or at most three suitably chosen tests are required to estimate the dependence of β_0 on the load; c is then estimated as the average of the test estimates. Once this is done, we can, on selecting suitable values for ϵ and z, employ eq. (45) for predictive purposes for an arbitrarily varying simple harmonic tensile load at any temperature. This predictive capability based on limited testing is a significant feature of engineering importance.

Many interesting points concerning the mean model merit exploration and discussion. Further, the variability inherent in the phenomenon must be brought into a model. We leave these matters for future papers.

REFERENCES

[1] A. Tobolsky and H. Eyring, Mechanical properties of polymeric materials. *J. chem. Phys.* **11**, 125–134 (March 1943).
[2] A. S. Krausz and H. Eyring, *Deformation Kinetics*. Wiley, New York (1975).
[3] S. N. Zhurkov, Kinetic concept of the strength of solids. *Int. J. Fracture Mech.* **1**, 311–323 (1965).
[4] C. B. Henderson, P. H. Graham and C. N. Robinson, A comparison of reaction rate models for the fracture of solids. *Int. J. Fracture Mech.* **6**, 33–40 (1970).
[5] H. Eyring, Viscosity, plasticity and diffusion as examples of absolute reaction rates. *J. chem. Phys.* **4**, 283–291 (1936).
[6] B. D. Colerman, Statistics and time-dependence of mechanical breakdown in fibers. *J. appl. Phys.*, **29**, 968–983 (1958).
[7] V. R. Regel and Leksovsky, A study of fatigue within the framework of the kinetic concept of fracture. *Int. J. Fracture Mech.* **5**, 99–109 (1967).
[8] S. J. Hudak, Development of standard methods of testing and analyzing fatigue crack growth data. AFML TR-18-40 (1978).
[9] D. A. Virkler, B. M. Hillberry and P. K. Goel, The statistical nature of fatigue crack growth. AFFDL TR-78-43 (1978).
[10] F. Kozin and J. L. Bogdanoff, Probabilistic models of fatigue in crack growth results and speculations. *Nuc. Energy Design* **115**, 143–171 (1989).
[11] M. Ichikawa, M. Hamaguchi and T. Nakamura, Statistical characteristics of m and C in fatigue crack propagation. *J. Soc. Mater. Sci.* **33**, 8–13 (1984).
[12] H. Ghonem and S. Dore, Experimental study of the constant probability crack growth curves under constant amplitude loading. *Engng Fracture Mech.* **27**, 1–25 (1987).
[13] D. W. Hoeppner and W. E. Krupp, Prediction of component life by application of fatigue crack growth knowledge. *Engng Fracture Mech.* **6**, 47 (1974).
[14] J. L. Bogdanoff and F. Kozin, *Probabilistic Models of Cumulative Damage*. Wiley, New York (1985).
[15] F. Seitz, *Modern Theory of Solids*, 1st edn., p. 3. McGraw-Hill, New York (1940).
[16] A. E. H. Love, *A Treatise on the Mathematical Theory of Elasticity*, 4th edn., p. 617. Cambridge University Press (1927).
[17] J. H. Weiner, *Statistical Mechanics of Elasticity*. Wiley, New York (1983).
[18] G. C. Shih and E. T. Moyer Jr, Path dependent nature of fatigue crack growth. *Engng Fracture Mech.* **17**, 769–780 (1983).

(*Received* 16 *October* 1989)

APPENDIX

In Fig. A1, we plot points from EN vs a and from EA vs n. These points come from the data analysis given in [10]. We observe that for all practical purposes the curves these sets of points lie on are the same curve. This justifies the use of EN vs a in the above data analysis instead of the EA vs n curve.

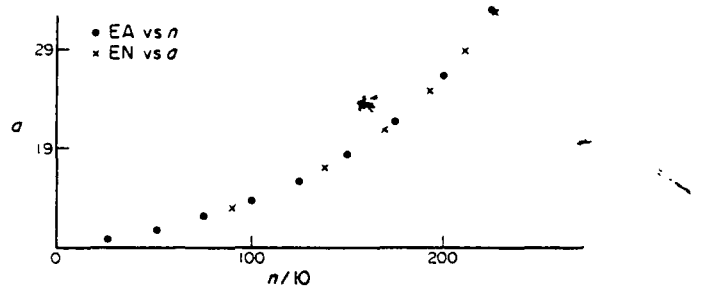

Fig. A1. A comparison of EN vs a points and EA vs n points for VHG data.

APPENDIX II

March 8, 1991

Cumulative Damage Model for Fatigue Crack Growth

based on

Reaction Rate Theory, II

by

F. Kozin[1]

J. L. Bogdanoff[2]

December 1990

---

(1) Deceased.

(2) Prof. Emeritus, School of Aero & Astro, Purdue University, W. Lafayette, Ind. 47907.

ACKNNOWLEDGEMENT

The authors wish to thank Dr. T. T. Soong, SUNY, Buffalo, for many discussions and helpful suggestions during the preparation of the manuscript.

This research is sponsored in part by AFOSR under Contract F49620-90-C-0059. The U.S. Government is authorized to reproduce and distribute requests for Governmental purposes not withstanding any copyright violation hereon.

Abstract

A study is continued of a macro model of FCG that is based upon a micro result from reaction rate theory. The previously presented deterministic (mean) model is examined further, and a probabilistic model is introduced. Analysis of fatigue crack growth (FCG) data for periodic tensile loads reveals that three material parameters are required. The model also explicitly contains the load and the temperature T. It is shown that T and the form of the periodic load are important quantities of which the former has interesting implications for accelerated testing. The minimum amount of testing required for predictive purposes is also discussed.

1. Introduction

We present in [1]* the derivation of a deterministic macro model of fatigue crack growth (FCG) based on a micro result from reaction rate theory along with an initial study of some of its properties. This presentation provides a brief survey of some of the interesting features of the FCG process and its modeling by this approach.

The purpose of the present paper is threefold: First, further studies of the deterministic (mean) model for the evolution of the dimensionless crack length are presented and discussed. We use for this purpose a data analysis of six sets of FCG in which the specimens are under simple harmonically varying tensile load. The studies indicate the importance of the model having three material parameters, one of which depends on the load. The model's explicit dependence on the temperature T and the wave form of the periodic load also indicates the importance of these two quantities in the evolution of the crack length.

Second, and initial study is made of how the ever present variability in FCG might be incorporated into the macro mean or deterministic model by means of random material behavior. A data analysis of the variability present in the data sets is employed to estimate the distributions of random material behavior, such distributions then producing the distributions of the time to reach a given crack length. The closeness of the standardized distributions of the random material behavior is discussed and suggests that there might be an underlying micro random material behavior that merits study.

Finally, we consider the minimum amount of testing required to estimate the macro model parameters for predictive purposes, and the most expeditious method for accelerating tests. Since only one material parameter depends on the load, it turns out that two or three tests at suitably chosen loads are needed for parameter estimation; then it is possible to predict the time

---

* Hereinafter referred to as Part I or simply as I.

to reach a given crack length over a wide range of loads. A standard method for accelerating fatigue and FCG tests is to increase the loads, which introduces the question of the effect of changed load interaction. The model indicates that testing time can be shortened by the simple expedient of increasing the temperature T with the same loads, which eliminates the load interaction question.

We begin by giving a short review of the derivation of the deterministic model.

We close with a conclusion section that summarizes the results of the study.

2. Brief Review of Deterministic Model

The basic specimen geometry under consideration is a thin center crack panel under axial tensile load F(t) (See Figure 1 of I). We start from the macro equations (8I) and (9I):

$$\frac{da}{dt} = \int_a^{l_o} \alpha e^{\beta s(t,\xi)} d\xi \,. \tag{1}$$

$$F(t) = 2w\int_a^{l_o} s(t,\xi) d\xi \,, \tag{2}$$

where

a = 1/2 crack length,

l_o = 1/2 panel width,

w = panel thickness,

ξ = distance from panel center line to a generic point in unbroken portion of crack plane,

$$\alpha = \frac{kT}{h} e^{-\frac{\Delta G^*}{kT}} \,, \quad \beta = \frac{\lambda}{vkT} \,, \quad T = \text{absolute temperature} \,,$$

k = Boltzmann's constant , h = Planck's constant ,

λ = average distance over which force acts in bond breaking , (3)

v = mean number of atomic bonds per unit area .

$s(t, \xi)$ is the normal stress on the unbroken portion of the crack plane at time t and location ξ; it is a bounded function. ΔG^* is a material parameter that can usually be estimated from existing information. The growth control parameter β or λ/υ depends on the material and how it is formed into components; it must be estimated from data.

Neglecting dynamical effects in the specimen, we can assume (see (16I))

$$s(t, \xi) = s(\xi)g(t)\,, \tag{4}$$

where the stress factor $s(\xi)$ only depends on ξ and $g(t)$ is a dimensionless multiplicative time factor depending on t and crack length.

The normal stress is high in the region of irreversible bond breaking just ahead of the crack tip and then decreases to an elastic stress as we move away from the crack tip in the crack plane. A realistic assumption for $s(\xi)$ is

$$\begin{aligned} s(\xi) &= \sigma_p \quad , \quad a \le \xi \le a + \Delta\,, \\ &= \sigma_e (< \sigma_p), \quad a + \Delta < \xi < l_o\,, \end{aligned} \tag{5}$$

(see (17I)). Other assumptions are possible (see (17bI)), but (5) is the simplest in view of the fact that (1) and (2) are not overly sensitive to the precise form of $s(\xi)$.

The substitution of (4) and (5) into (1) and (2) yields

$$g(t) = \frac{s_o(t)/\sigma_e}{1 - y - \delta + r_\sigma \delta} \tag{6}$$

$$\frac{dy}{dt} = \alpha \left[\delta e^{\frac{\beta r_\sigma s_o(t)}{1-y-\delta+r_\sigma\delta}} + (1 - y - \delta) e^{\frac{\beta s_o(t)}{1-y-\delta+r_\sigma\delta}} \right], \tag{7}$$

where $s_o(t) = F(t)/2wl_o$ is the far field axial tensile stress, $y = a/l_o$ is the dimensionless crack length, $\delta = \Delta/l_o$ is the dimensionless length of the high stress region in the crack plane, and $\sigma_p/\sigma_e = r_\sigma = 1 + \epsilon$ is the ratio of the high stress to the elastic stress and is greater than one. Of course, $1 - y - \delta + r_\sigma\delta > 0$ and $0 < y < 1$.

Given α, β and $s_o(t)$, (7) must be integrated to yield y as a function of time. However, for the specific form of $s_o(t)$ we shall assume, a difference form of (7) is satisfactory for our purposes.

Let the far field axial stress $s_o(t)$ acting on the specimen be

$$\begin{aligned} s_o(t) &= \bar{s}_o + \Delta s \sin \omega t \text{ , or} \\ &= \bar{s}_o + \Delta s h(\tau) \text{ ,} \end{aligned} \tag{8}$$

where $\tau = \omega t$, $h(\tau)$ is continuous and periodic with period 2π, $|h(\tau)| \le 1$, it is odd with respect to π, so its mean value is zero, and $\bar{s}_o$ and $\Delta s > 0$. Let us discretize the crack length $a_o < a_1 < \cdots < a_n < l_o$, and time $0 < t_1 < \cdots < t_n$, where t_j is the mean time to reach a_j. Further, let us set

$$\begin{aligned} y_j &= a_j / l_o \quad , \\ \bar{y}_j &= (y_{j-1} + y_j)/2 \quad , \\ \Delta y_j &= y_j - y_{j-1} \quad , \\ \Delta t_j &= t_j - t_{j-1} \quad , \end{aligned} \tag{9}$$

where Δt_j in the time required for y to increase by Δy_{j-1}. The difference form of (7) that we employ here is

$$\Delta y_j = \alpha \Delta t_j \left[\delta_j e^{v_j r_\sigma \bar{s}_o} \frac{1}{2\pi} \int_o^{2\pi} e^{v_j r_\sigma \Delta s h(\tau)} d\tau + (1 - \bar{y}_j - \delta_j) e^{v_j \bar{s}_o} \frac{1}{2\pi} \int_o^{2\pi} e^{v_j \Delta s h(\tau)} d\tau \right], \tag{10}$$

where $v_j = \beta_j / (1 - \bar{y}_j - \delta_j + r_\sigma \delta_j)$, ω converts cycles Δn_j to time Δt_j.

The parameters r_σ and δ describe how the assumed form of the normal stress on the crack plane evolves with time. It is possible that y, r_σ, and δ form a state vector if we have differential equations describing the joint evolution of y, r_σ, and δ. This would imply that y is history dependent. However, at this time, we have no such evolutionary equations for these quantities. Therefore, to proceed with a study of (10) in conjunction with data we introduce the constraints

$$r_\sigma = 1 + \varepsilon\ ,\ \varepsilon = \text{constant} > 0\ ,$$

$$\delta_j = z\bar{y}_j\ ,\ z = \text{constant with } 0 < z < 1\ . \tag{11}$$

The first constraint says that as σ_e increases with increasing y σ_p also increases at the same rate. The second constraint says that the length of the high stress region of irreversible bond breaking in the crack plane increases as y increases. These statements are consistent with the qualitative behavior of a work hardening material. Eq. (11) are among the simplest that can be introduced but can be changed if necessary. More will be said about (11) when confronting data.

If $\varepsilon > .20$, parameter estimation studies reported in I and reported here indicate that the second term in the square bracket of (10) is negligibly small in comparison with the first term. Thus, (10), when combined with (11) can be written as

$$\Delta y_j = \alpha z \bar{y}_j \Delta t_j e^{v_j(1+\varepsilon)\bar{s}_o} \frac{1}{2\pi}\int_o^{2\pi} e^{v_j(1+\varepsilon)\Delta sh(\tau)} d\tau\ . \tag{12}$$

We consider two forms of $h(\tau)$, namely

$$h(\tau) = \sin\tau\ ,$$

$$h(\tau) = \frac{2\tau}{\pi}\ ,\ 0 \le \tau \le \pi/2\ ,$$

$$= 2 - \frac{2\tau}{\pi}\ ,\ \pi/2 \le \tau \le 3\pi/2\ , \tag{13}$$

$$= -4 + \frac{2\tau}{\pi}\ ,\ 3\pi/2 \le \tau \le 2\pi\ ,$$

The second form is a "saw-tooth" version of the first each having amplitude 1. First, consider the first of (13); then

$$\frac{1}{2\pi}\int_o^{2\pi} e^{x\sin\tau}d\tau = I_o(x)\,, \tag{14}$$

where $I_o(x)$ is the modified Bessel function of order zero. For the data studied, x is large; thus we can employ the approximation [2]

$$I_o(x) \doteq \frac{e^x}{\sqrt{2\pi x}}\,,\ x = \frac{(1+\varepsilon)\beta_j\Delta s}{1-(1-z\,\varepsilon)\bar{y}_j} \tag{15}$$

Hence, we can approximate (12) by means of

$$\Delta y_j = \alpha z\bar{y}_j\Delta t_j(2\pi u_j\Delta s')^{-1/2}e^{u_j}\,,\ \text{or}\ \Delta t_j = (\alpha z\bar{y}_j)^{-1}\Delta y_j(2\pi u_j\Delta s')^{1/2}e^{-u_j} \tag{16}$$

when Δs is not too small (e.g. $x \geq 10$), and

$$\begin{aligned} u_j &= \frac{(1+\varepsilon)\beta_j\bar{s}_o'}{1-(1-z\,\varepsilon)\bar{y}_j}\,, \\ \bar{s}_o' &= \bar{s}_o + \Delta s\,, \\ \Delta s' &= \Delta s/\bar{s}_o'\,. \end{aligned} \tag{17}$$

Next, consider the second form of $h(\tau)$ given in (13). Then, under the same type of approximation we find

$$\Delta y_j = \frac{\alpha z\bar{y}_j\Delta t_j}{2}(u_j\Delta s')^{-1}e^{u_j}\,, \tag{18}$$

where (17) still holds. We assume in Part I that $h(\tau)$ = rectangular wave form with the area under the half-wave equal to the area under $\sin\tau$ for $0 \leq \tau \leq \pi$. The equation corresponding to (16) and (18) then becomes

$$\Delta y_j = \frac{\alpha z\bar{y}_j\Delta t_j}{2}e^{u_j}\,, \tag{19}$$

which is (31I) if $z = 1/4$, and $\bar{s}_o' = \bar{s}_o + \frac{4}{\pi}\Delta s$, $\epsilon = 1$. In (18) and (19), Δs is not too small

Equations (16), (18), and (19) are based on the step distribution for the stress $s(\xi)$ given by (5). Another possible choice is given by (17bI); still other reasonable possibilities exist. However, at this point in the study, use of (5) is appropriate because of its simplicity.

The material parameters in (16), (18), and (19) are α and β; $\in$ and z are geometrical parameters connected with (5). We have already stated that the parameter α (or ΔG^{+}) can be estimated from known results (See Zhurkov [3]). However, the β_j must be estimated from data. The selection of values for $\in$ and z will be discussed below.

Let us consider how $\beta_j \bar{s}_o'$ will be estimated from data, using (16). From the data, we can find for each Δy_j $\Delta t_j = E\{\Delta T_j\}$, where ΔT_j is a random variable representing the time for the crack to increase by Δy_j in dimensionless length. Then, write (16) as

$$\frac{\Delta y_j \sqrt{2\pi}}{\alpha z \bar{y}_j \Delta t_j} = \frac{e^{u_j}}{\sqrt{u_j \Delta s'}} \tag{20}$$

On taking logarithms, we obtain

$$b_j = \frac{1}{2}\log 2\pi + \log\frac{\Delta y_j}{\alpha z \bar{y}_j \Delta t_j} = u_j - \frac{1}{2}\log u_j \Delta s' . \tag{21}$$

Set

$$u_j = b_j + d_j \tag{22}$$

It follows from (21) that

$$d_j = \frac{1}{2}\log b_j \Delta s' + \frac{1}{2}\log\left(1 + \frac{d_j}{b_j}\right) \tag{23}$$

and since d_j/b_j is small for the data considered

$$d_j \simeq \left(1 - \frac{1}{2b_j}\right)^{-1} \frac{1}{2}\log b_j \Delta s' \tag{24}$$

Thus, we have an estimate for u_j. We then find an estimate for $\beta_j \bar{s}_o'$ by employing the first of (17)

$$\beta_j \bar{s}_o' = \frac{1-(1-z\,\varepsilon)\bar{y}_j}{1+\varepsilon} u_j \,, \tag{25}$$

once z and $\in$ are selected. Similar results can be obtained for (18). We easily find from (19) that

$$u_j = \log \frac{2\Delta y_j}{\alpha z \bar{y}_j \Delta t_j} \,, \tag{26}$$

which gives an estimate for u_j in this case; estimates for $\beta_j \bar{s}_o'$ again follow from (25).

Eq. (7) is the basic contribution in this paper (and I). It contains the significant quantities of engineering interest. Comparison with two other models of FCG based on reaction rate theory will be commented upon in Section 4.

3. Parameter Estimates for Deterministic Model

We employ the same experimental data on FCG that is considered in I, namely

a) ASTM E24.04.01 Round Robin Data [4]

The material is 10Ni8Co1Mo steel, 24 replications, $\omega = 10\pi$ rad/sec.

b) VHG Data [5]

The material is 2024-T3 al alloy, 68 replications, $\omega = 40\pi$ rad/sec.

c) IHN Data [6]

The material is 2024-T3 al alloy, 30 replications, $\omega = 36.8\pi$ rad/sec.

d) GD Data [7], 3 load conditions, $\omega = 20\pi$ rad/sec.

The material is 7075-T6 al alloy, 60 replications for each load condition.

Let $t_{j,k}$ be the time to reach crack length a_j for sample k in one experiment, where $k = 1, \cdots, n$. Then, with

$$\Delta t_{j,k} = t_{j,k} - t_{j-1,k}\,, \tag{27}$$

we employ

$$\Delta t_j = \frac{1}{n}\sum_{k=1}^{n} \Delta t_{j,k} \tag{28}$$

as the (mean) time required for the crack length to increase from a_{j-1} to a_j or to increase by amount $\Delta a_j = a_j - a_{j-1}$. Thus, for each load condition, we have Δt_j and Δy_j at a number of crack length.

We employ (16) for parameter estimation since in all experiments $h(\tau) = \sin \tau$. In b), the controlled ambient air temperature is 297°K and we assume a 10°C rise in specimen temperature due to material hysteresis at 20 Hz, producing an assumed steady state T = 307°K. In a), c), and d), we assume as a reasonable value the temperature T = 300°K.

The ΔG^{-} value in each experiment is given in Part I. Thus, for each experiment, we have an estimate for α from the formula given in (3), and needed in (16).

The quantities $\bar{s}_o'$ and $\Delta s'$ are obtained from the load condition and specimen geometry for each experiment by means of the second and third of (17); these quantities are also needed in (16).

It follows that given the $(\Delta t_j, \Delta y_j)$ (16) provides the estimates for the parameters $\beta_j \bar{s}_o'$, for the selected values of z and ε; then, we get the β_j from these estimates.

WOL specimens are employed in data set a), whereas in the other data sets the specimens are center crack panels. Since significant bond breaking only occurs in the high stress region, we will employ the results in Section 2 for this case even though r_σ and σ_e must be viewed in a different manner than for center crack panel specimens.

The general nature of the parameter estimates $\beta_j \bar{s}_o'$ found here is of the same as found in Part I, where we assumed $h(\tau)$ = rectangular wave form. That is, in the data sets of b), c), and d), there is an initial deviation of the $\beta_j \bar{s}_o'$ from a straight line with negative slope, which we ascribed in I to transient material behavior; no such deviation from a straight line occurs in data set a). Thus, only a few of the graphs presented in I will be repeated here. Instead, we confine attention to the expression for the straight line approximation to the estimates.

a) E24.04.01 Data

Figure 1 shows the parameter estimates $\beta_j \bar{s}_o'$ from Part I where $h(\tau)$ = rectangular and the estimates from (18), both with $\epsilon = 1$ and $z = 1/4$. The crack length increases from 1 in. to 2 in. and, with $\Delta a_j = .05$ in., this produces twenty a_j; $l_o = 2.55$ in. and we assume $T = 300°K$. The straight line approximations differ by a significant amount. The mean square (ms) approximate lines obtained with the use of (18) for estimating the $\beta_j \bar{s}_o'$ is

$$\beta_y \bar{s}_o' = 59.534265\ (1 - .723460\ y)\,, \tag{29}$$

where $\bar{s}_o' = 1725.49$ psi and $\Delta s' = .450000$. The corresponding equation from I is

$$\beta_y \bar{s}_o' = 59.2759\ (1 - .73625\ y) \tag{30}$$

As noted above, there is no deviation of the estimates from a straight line when starting at $a_o = 1$ in. and ending at $a_n = 2$ in. even though at the end point the crack tip is close to the specimen boundary.

b) VHG Data

The straight portion of the estimates is from crack length 16 mm. - 37 mm. (Δa_j = 1 mm.), 37 mm. - 44.2 mm. (Δa_j = 1.2 mm.), 44.2 mm . - 49 mm. (Δa_j = 1.6 mm.), and 49mm-49.8mm (Δa_j = .8 mm.), giving 31 values for $\bar{a}_j$, l_o = 76.2 mm. so that $\bar{y}_j = \bar{a}_j/76.2$ and $\Delta y_j = \Delta a_j/76.2$, T = 307°K. The ms. approximate line is

$$\beta_y \bar{s}_o' = 25.952791\,(1 - .725106\,y)\,, \tag{31}$$

where $\bar{s}_o'$ = 8,766.67 psi, $\Delta s'$ = .401141, ϵ = 1, and z = 1/4. The initial portion from 9 mm. - 16 mm. provides estimates that deviate from a straight line in the same manner as shown in Figure 4 and 5 in Part I. The equation from I corresponding to (31), when $h(\tau)$ has a rectangular wave form, is

$$\beta_y \bar{s}_o' = 26.20280\,(1 - .72878y) \tag{32}$$

Thus, there is no reason for graphing the estimates.

In the first crack length interval 16 mm. - 37 mm., we use Δa_j = 1mm.. However, the data in that interval are given at Δa_j = .2 mm.. This provides an opportunity for checking on whether or not use of smaller Δy_j produces a significant difference in the ms. approximate line. On comparing the ms. approximate lines in the interval 16 mm. - 36 mm., using Δa_j = 1 mm. and .2 mm., we find that the numerical values in the ms. approximate lines differ by a maximum of .04%. It thus appears that using smaller Δy_j does not produce a significant difference in the parameter estimates. However, a bigger difference in parameter values appears when the Δa_j were changed from 1.0 mm. to 2 mm. Thus, the magnitude of Δa_j should not be too large.

c) IHN Data

The straight portion of the estimated $\beta_j \bar{s}_o'$ is for $\bar{a}_j = 9$ mm., 11 mm., $\cdots$, 21 mm., with $\Delta a_j = 2$ mm., giving 7 points. $l_o = 35$ mm. and T = 300°K. The ms. approximate straight line is

$$\beta_y \bar{s}_o' = 26.667678\ (1 - .723869\ y)\ , \tag{33}$$

where $\bar{s}_o' = 10{,}814$ psi, $\Delta s' = .397633$, $\epsilon = 1$, $z = 1/4$. The estimates are obtained using (16) and the $(\Delta y_j, \Delta t_j)$ are obtained from the data. The estimates at $\bar{a}_j = 7.5$ mm. deviates from the straight line (33) as is the case in I (See Figure 6 of I).

d) GD Data

We assume $\epsilon = 1$ and $z = 1/4$. In Part I (see Figure 7 I), we employ six $\bar{a}_j$. Here we use 24 $\bar{a}_j$ covering the same range of crack lengths for the three load conditions as in I. $l_o = 50.8$ mm. and $T = 300°K$. The 24 $\beta_j \bar{s}_o{}'$ estimates are obtained using (16). Figure 2 shows the $\beta_j \bar{s}_o{}'$ estimates for the three load conditions.

The first five estimates show transient material behavior in each case. The ms. approximate straight lines for the straight position are, using 19 $\bar{a}_j$ in each case,

$$\begin{aligned} GD^{\#}1 &: \beta_y \bar{s}_o{}' = 26.712158\,(1 - .722287\,y)\,, \\ GD^{\#}2 &: \beta_y \bar{s}_o{}' = 26.954427\,(1 - .727481\,y)\,, \\ GD^{\#}3 &: \beta_y \bar{s}_o{}' = 26.518554\,(1 - .722104\,y)\,, \end{aligned} \tag{34}$$

where

$$\begin{aligned} GD\#1 &: \bar{s}_o{}' = 10{,}246 \text{ psi}\ ,\ \Delta s' = .199883\,, \\ GD^{\#}2 &: \bar{s}_o{}' = 10{,}004 \text{ psi}\ ,\ \Delta s' = .249900\,, \\ GD^{\#}3 &: \bar{s}_o{}' = 6{,}830 \text{ psi}\ ,\ \Delta s' = .299854\,. \end{aligned} \tag{35}$$

Equations (34) and (35) produce

$$\begin{aligned} GD^{\#}1 &: \beta_o = .00260708\,, \\ GD^{\#}2 &: \beta_o = .00269436\,, \\ GD^{\#}3 &: \beta_o = .00388265\,. \end{aligned} \tag{36}$$

The form of (34) is

$$\beta_y \bar{s}_o{}' = \beta_o \bar{s}_o{}'(1 - cy) \tag{37}$$

The average value of c is .723957, with a maximum deviation of .4867%. It appears that c does not depend strongly on the load condition. This same observation was noted in I where $h(\tau) =$ rectangular wave form.

We observe from (36) that β_o does depend on the load condition, as it does in I. Figure 3 shows β_o plotted against $\bar{s}_o'$. With this location of the points it is not possible to determine the precise nature of the functional dependence. However, with test conditions that provide well spaced points on the $\bar{s}_o'$ this should be possible.

It follows that with two or three suitably chosen test load conditions we can find the average value of c and obtain a graph for β_o as a function of $\bar{s}_o'$. Then, with (9) and (20), we can predict Δt_j, as a function of $(\Delta y_j, \bar{y}_j)$ for other load conditions for $h(\tau) = \sin \tau$, $\epsilon = 1$, $z = 1/4$, and constant or variable T, and also find $t_j = \Delta t_1 + \cdots + \Delta t_{j-1}$ as a function of y_j.

We now take up a number of interesting points not previously considered. First, using the IHN Data, let us consider the effect on the $\beta_j \bar{s}_o'$ estimates when ϵ takes different values with the same $\delta = .25$ y. We only consider the straight portion of the $\beta_j \bar{s}_o'$. Figure 4 shows the results for $\epsilon = \sigma_p/\sigma_e - 1$ equal to .25, .50, and 1.0. The straight line character of the estimates still obtains in each case. Reducing ϵ causes the numerical values of the $\beta_j \bar{s}_o'$ to increase. Our assumption throughout the data analysis that $\epsilon = 1$ is reasonable, although a closer connection with how the form of $s(t, \xi)$ evolves with time, based on experimental evidence, is certainly needed.

Next, let us hold ϵ constant and change δ. Figure 5 assumes $\epsilon = 1$ and δ is changed. As long as we assume $\delta = zy$, we see that the straight line character of the estimates still obtains. However, if δ = constant, the straight line approximation is no longer satisfactory. We know that the length of the high stress zone in the crack plane increases for materials that work harden. Thus, the choice $\delta = zy$ is reasonable in this study. Again, experimental evidence on how $s(t, \xi)$ evolves with time is needed.

Equations (16), (18), and (19) contain the temperature T explicitly. Let us consider how T influences the results predicted by the model. We employ the VHG Data for this purpose.

We have from (3)

$$\alpha = \frac{kT}{h} e^{-\frac{\Delta G^*}{kT}} \quad , \quad \beta_o = \frac{\hat{\lambda}_o}{\upsilon kT} \; ; \tag{38}$$

$T_o = 307°K$ for the data. We assume $\epsilon = 1$ and $z = 1/4$ and employ the same numerical values for the other quantities as previously used when making parameter estimates in b).

Let $T_1 = 312°K$ and $T_2 = 302°K$. We find using (31) and (38) that

$$\begin{aligned} T_1 = 312°K : \alpha &= 4.73250 \times 10^{-25} \quad , \quad \beta_j \bar{s}_o' = 25.5369\,(1 - .725106\,\bar{y}_j)\,, \\ T_0 = 307°K : \alpha &= 1.15670 \times 10^{-25} \quad , \quad \beta_j \bar{s}_o' = 25.9528\,(1 - .725106\,\bar{y}_j)\,, \\ T_2 = 302°K : \alpha &= 2.69906 \times 10^{-26} \quad , \quad \beta_j \bar{s}_o' = 26.3826\,(1 - .725106\,\bar{y}_j)\,. \end{aligned} \tag{39}$$

Notice that we assume the coefficient of y inside parenthesis and also λ_o do not depend on T. We use (16) and $\beta_j \bar{s}_o'$ from (39) to predict Δt_j as a function of Δy_j or $\bar{y}_j$, starting at crack length 16 mm with $\Delta a_j = 1$ mm and ending at crack length 36 mm. This interval 16 mm. - 36 mm. is in *the straight portion of the* $\beta_j \bar{s}_o'$ estimates. We could have started at 9 mm. if we were willing to employ graphical results instead of (32).

The solid curves in Figure 6 are from prediction at the indicated temperatures, and the solid "dots" are from the data. Two points are worth noting. First, as we expect, the model predictions at $T = 307°K$ are in excellent agreement with the data. Second, the predicted Δt_j at $T = 302°K$ and $312°K$ are substantially different from the data even though the temperature difference is only $\pm 5°K$; this is due to the fact that while the temperature difference is small and the change in the $\beta_o \bar{s}_o'$ is small, small differences in the $\beta_o \bar{s}_o'$ produce large differences in predicted Δt_j because $\beta_o \bar{s}_o'$ appears in the exponent. We do not have data with which to validate either prediction. However, the experiments of Zhurkov [3] on time to failure under static load do indicate that these times are sensitive to small temperature changes. The results in Figure 6 imply that unless the temperature is carefully controlled at a constant value or is accurately measured throughout the experiment the data will be of little value for model validation. *Further, prediction of life behavior in a component* (regardless of which model is employed) must account for temperature if accurate results are to be expected. There is another

possible aspect of temperature behavior that we must consider when experiments are performed.

We speculated in Part I that the transient behavior observed at the start of the $\beta_j \bar{s}_o'$ estimates, shown for example in Figure 2 might be due solely to material behavior. However, examination of [5] suggests this may not be the case.

Considerable care was taken in the VHG experiments mean of by a suitable load shedding program to eliminate the effect of transient material behavior due to the rapid starting of the crack. Thus, this type of transient material behavior is not likely the source of the transient $\beta_j \bar{s}_o'$ estimate behavior observed.

We note that in the VHG experiments desiccated air was employed and the room temperature was controlled at 24°C. At a frequency of 20 Hz, we know the specimen temperature will rise above 24°C until a steady value is reached, and we assume this rise is 10°C, giving T = 307°K. It follows that in the VHG Data the observed transient behavior of the $\beta_j \bar{s}_o'$ estimates is most likely due to the transient temperature behavior; this also is most likely the case for the IHN Data and the GD Data. However, to definitely confirm this view it is necessary to measure the specimen temperature at several points, particular by just ahead of the crack tip in future experiments.

Figure 7 is concerned with the effect of the form of the periodic function $h(\tau)$ on the Δtj. To study this effect, we again employ the VHG Data with T = 307°K. The solid curve on the left is for $h(\tau) = \sin \tau$, and is the same as the middle curve in Figure 6. We have no experimental evidence to support the assumption that the numerical values in (32) are independent of the wave form in $h(\tau)$. However, let us assume this assumption is correct. Let us assume $h(\tau)$ is given by the second of (13). Then, we must employ (18), and predict Δt_j for the Δy_j from

$$\Delta t_j = \frac{2\Delta y_j}{\alpha z \bar{y}_j}(u_j \Delta s')e^{-u_j}, \tag{40}$$

with $\in = 1$, $z = 1/4$, and the $\beta_j \bar{s}_o'$ from (32). The lower solid curve in Figure 7 is predicted. The difference in the two curves is substantial. However, since

$$|\sin\tau| \geq |h(\tau)|\ ,$$

where $h(\tau)$ is the "sawtooth" form, the difference is to be expected. Again we have no experimental data with which to validate the prediction shown in Figure 7.

We have already observed that small changes in $\beta_o \bar{s}_o'$ due to small temperature changes produce much larger changes in the predicted Δt_j because this term appears in the exponent. Actually, we see from (40) that any change in the u_j given by the first of (17), even by small amounts, produces substantial changes in the predicted Δt_j. This is one source of sensitivity in the model. On the other hand, when the form of $h(\tau)$ is changed from $\sin\tau$ to "sawtooth," u_j does not change; rather the coefficient of e^{-u_j} changes. At $T = 307°K$, we find for the VHG data in the 16 mm. - 36 mm. range with $\Delta a_j = 1$ mm.

$$\frac{(\Delta t_j)^{\text{sawtooth}}}{(\Delta t_j)^{\sin\tau}} = .797884\sqrt{u_j \Delta s'}\ , \tag{41}$$

and, with $\Delta s' = .401141$, and $u_j \doteq 52.5$, this ratio equals 3.66. Thus, the predicted Δt_j also are sensitive to the reasonably small change in the wave form.

Next, let us observe how we must proceed if we wish to predict t_j with different $\bar{s}_o$ and Δs. Consider the GD Data. It is clear from (37) that we must estimate β_o and c. We take for c the average value .723957, since c does not appear to depend on $\bar{s}_o$ and $\Delta s > 0$. To estimate β_o for the selected $\bar{s}_o$, Δs, and $\bar{s}_o' = \bar{s}_o + \Delta s$, we assume that it suffices to approximate the β_o values in (36) by the curve

$$\beta_o = \frac{6.714138}{10^3} - \frac{.442001}{10^6}\,\bar{s}_o' + \frac{.00401678}{10^9}\,(\bar{s}_o')^2 \tag{42}$$

For the selected $\bar{s}_o'$, we estimate β_o from this equation assuming $\bar{s}_o'$ is either in or not to far outside the interval (6830, 10246) given in (35). We then employ (16) in the form

$$\Delta t_j = \frac{\Delta y_j}{\alpha z \bar{y}_j} (2\pi u_j \Delta s')^{1/2} e^{-u_j} , \tag{16'}$$

and u_j from (17) and (37) with $\epsilon = 1$, $z = 1/4$ to predict the t_j since all quantities are now known.

If Δs (or $\Delta s'$) is small, the approximation (15) will not be satisfactory. Then, we replace (16') by

$$\Delta t_j = \frac{\Delta y_j e^{-u_j'}}{\alpha z \bar{y}_j} \left[I_o \left\{ \frac{\beta_j r_\sigma \Delta s}{1 - (1 - \epsilon\, z)\bar{y}_j} \right\} \right]^{-1} ,$$

or, more generally,

$$\Delta t_j = \frac{\Delta y_j e^{-u_j'}}{\alpha Z \bar{y}_j} \left[\frac{1}{2\pi} \int_o^{2\pi} e^{\frac{\beta_j r_\sigma \Delta s}{1-(1-\epsilon\, z)\bar{y}_j} h(\tau)} d\tau \right]^{-1} , \tag{43}$$

where $u_j' = \beta_j r_\sigma \bar{s}_o / \{1 - \epsilon\, z)\bar{y}_j\}$. We note that if $\Delta s = 0$, i.e. a constant stress, (43) because

$$\Delta t_j^{(s)} = \frac{\Delta y_j e^{-u_j'}}{\alpha z \bar{y}_j} , \tag{44}$$

which predicts the time $\Delta t_j^{(s)}$ required for the crack to increase by the dimensionless amount Δy_j under a static far field tensile stress $\bar{s}_o$. Clearly, the $\Delta t_j^{(s)}$ in (44) will be much larger than the Δt_j in (16') if Δs is appreciably greater than zero. We observe that the second factor on the right of (43) represents the effect of Δs in reducing $\Delta t_j^{(s)}$ to Δt_j. Since we know β_j depends on $\bar{s}_o$ and Δs according to the GD Data, and since we have no data for the static load case, we cannot say how the β_j in (16') relate to the β_j in (44).

It follows from the material presented in this Section that the data analysis and study conducted reveal useful information about the model and its predictive capabilities, and the FCG process. It also is clear that there are gaps in the data base needed to validate the proposed

deterministic model.

4. Discussion of Deterministic Model

We consider FCG as a chemical process in which irreversible atomic bond breakage is responsible for the growth of the macro observable crack length and for which rate reaction theory provides the basis for macro modeling starting at the micro level. The problem we face is how to proceed from the micro level to the macro level when there is at least one observable. Given the specimen geometry, a periodic tensile load F(t), and this point of view, let us consider the bond breaking on the crack plane in order to review how we approach this problem.

The atomic bond breaking process on the crack plane is complex. An elementary picture of this process is as follows: In the immediate region to the right of the crack tip at a, irreversible atomic bond breaking due to the external load is the dominant process. In the next region on the right, bonds are broken by the external load, but an equivalent number of new bonds are established producing plastic deformation as the dominate process. Only the thermal type of bond breaking and healing occurs in the next region on the right; this is the region of elastic material behavior. We model this elementary picture in the following simple manner.

First, we assume we can approximate the mean bond force f by employing the average macro concept of normal stress $s(t, \xi) = s(\xi)g(t)$, where $g(t)$ is a dimensionless time factor depending on F(t) and the crack plane geometry, and $s(\xi)$ and $g(t)$ are bounded functions. Second, we elect to divide the atomic bond breaking process into a region just to the right of the crack tip in which there is only irreversible bond breakage, and a region to the right of the first region in which the amount of irreversible bond breakage is negligible, disregarding all other types of bond behavior. Based on the micro result (1I) from reaction rate theory for the mean rate

$$\kappa_b = \frac{kT}{h} e^{-\frac{\Delta G^* - \lambda f}{kT}}, \quad f = s(t, \xi)/\upsilon . \tag{45}$$

of single bond breakage, we can achieve this picture of the process by taking the stress factor $s(\xi)$ on the crack plane to have the form given by (5), where $\sigma_p > \sigma_e$ and $\sigma_p/\sigma_e = r_\sigma > 1.2$. The

expression for κ_b assumes there is only a single energy barrier that must be crossed for atomic bond breakage and there is no bond healing. Clearly, other more complex assumptions can be adopted to achieve the above picture of the bond breaking process; further, the simplified picture of the bond breaking process can be enriched in various ways.

The form (4) assumes there are no dynamical effects induced by the testing procedure, and this is usually the case.

The macro equations (1) and (2) are based only on our picture of the bond breaking process for the situation under consideration. On combining these equations with (3), (4) and (5), we obtain (6) and (7). Equation (7) is one of our major contributions, and is a different form for FCG than provided by other approaches; this equation is interesting for several reasons.

First, it is based on physical principles and the assumption that the mean bond force f can be approximated by employing the normal stress $s(t, \xi)$ on the crack plane.

Second, besides the dimensionless crack length y, the quantities δ and r_σ from (5) evolve with time. This opens up the possibility that y, δ, and r_σ may constitute a state vector if we can find their joint evolutionary equations. This possibility has not previously been considered. We do not have such joint evolutionary equations at this time, however. Thus this interesting possibility cannot be considered further.

Third, (7) contains explicitly the temperature T, and the load F(t) through the far field tensile stress $s_o(t)$. Thus, (7) contains quantities of direct engineering interest that help define the environment.

Fourth, (7) contains explicitly the material parameters α (or ΔG^+) and β as defined by (3). ΔG^+ is a free energy; it is a thermodynamic quantity whose value either can be estimated once for all for the material from tabulated data on the heat of sublimation (see Zhurkov [3] and Krausz-Eyring [8]) or it can be estimated from simple static tests (see Zhurkov [3]). On the other hand, the growth control material parameter β, which we find depends on y, defines the strength of the material; it depends on how the material is formed into components and must be estimated by means of appropriate test data. Thus, (7) contains material parameters of direct

engineering interest.

Fifth, the alternative form of $s(\xi)$ given in (17bI) admits the possibility that the highest stress is at the crack tip. This means that even if $\Delta\sigma$ is small the maximum rate of bond breakage will occur at the crack tip, which is physically appealing. This point is discussed in Part I (see eq. (19bI)), where we note that if $\Delta\sigma/\sigma_e$ is small, the form of (7) remains unchanged. Thus, (7) still applies in this more general and physically appealing situation.

Sixth, inspection of the integral in (12) suggests that there might be different $h(\tau)$ that will give the same value to the integral; i.e. different wave forms will produce the same damage accumulation process if

$$\frac{1}{2\pi}\int_o^{2\pi} e^{xh(\tau)}d\tau$$

is the same for different $h(\tau)$ and all $x > 0$. Given the conditions assumed for $h(\tau)$ plus the continuity conditions imposed by the fact that it is a physical load, it can be shown this is not possible, if, in addition, $h(\tau)$ is monotone increasing (or decreasing) on the interval $(-\frac{\pi}{2}, \frac{\pi}{2})$ as is the case when $h(\tau)$ is given by (13). If this monoticity condition is not satisfied, however, different $h(\tau)$ will produce the same value for the integral; while this situation has interesting implications, we will not discuss it here.

Finally, if there is a chemical reaction involved, such as corrosion, it will enter (7) through the growth control parameter β. Now let us turn to how (7) is employed in conjunction with FCG data.

The integration of (7) requires that we assume a specific form for $s_o(t)$; we take $s_o(t)$ to be tensile and periodic in t as specified in (8). Further, since we do not have joint evolutionary equations for y, δ, and r_σ at this time, we assume the constraint equations (11) for δ and r_σ. The combination of (7), (8), and (11) produces

$$\frac{dy}{dt} = \alpha z y e^{\frac{\beta_y r_\sigma (\bar{s}_o + \Delta sh(\omega t))}{1-(1-\epsilon z)y}} , \qquad (46)$$

since if $r_\sigma > 1.2$, the second term on the right of (7) can be ignored. Even with these choices, the exact integration of (46) is difficult. However, the use of different forms for the periodic element $h(\tau)$ in (8), for example (13), makes possible the approximate integration of (46) in the difference forms (16), (18), and (19) for the deterministic development of FCG in discretized t and y; this step is reasonable since y only changes by small amounts for all Δt_j involved.

The selection of the constraint equations is based on what we know about the general behavior of FCG in ductile polycrystaline metals, as already noted, and simplicity. Experimental evidence must ultimately be employed to determine if the choice is consistent with the facts. Further, if (11) is a reasonable choice, it is then necessary to determine on the same basis if our choice $\varepsilon = 1$ and $z = 1/4$ is reasonable. Such experiments would be different from those usually conducted in FCG. In addition, these experiments would have to measure the temperature T as we have found it to be important parameter.

We now wish to comment on two other models of FCG that originate in reaction rate theory. Yokobori and co-workers [10] have since the mid 1950's applied reaction rate theory to fracture, fatigue, and FCG, producing many interesting results; we note in particular [11]. Another effort in this direction for FCG is given in [12]. Each introduces crack length and load in a different manner than we do. In [12], for example, fracture mechanics based quantities are introduced in place of the λf-term in the exponent of (1I) or (45) which is physical questionable. Each contains one material parameter equivalent to our α. Each contains a second material parameter similar to our β; however, neither group investigated to determine if this parameter depends on crack length. We have found in our formulation that β depends on y and this dependence is essential for predictive accuracy. It therefore appears that our method for introducing crack length and load (stress) has advantageous not possessed by these two models.

We assume the periodic form (8) for $s_o(t)$ because this is the case for the available data. However, it is clear that in (7) there is no mathematical restriction on $s_o(t)$ beyond being a

positive bounded contin· ous function, oscillatory or not. For example, $s_o(t)$ can be an oscillatory non-periodic function such as provided by a sample function from spectrum loading. But, we must then confront the possibility that hi-lo vs. lo-hi loads may produce different amounts of physical damage accumulation than predicted mathematically by (7) due to the load history dependence in the material [9]. Put another way, the growth control parameter β may depend on load order. Without experimental evidence to lend support, predictions of FCG based on (7) for any such $s_o(t)$ must be viewed with caution.

The model consider so far is deterministic. The data analysis employs the pair of quantities Δy_j and Δt_j. Δy_j is specified by the choice of the division a_j of the crack length employed. The time t_j to reach a_j depends on the sample selected in a test, and these times vary in a random manner. Let the random variable T_j denote this random time. We assume for a deterministic model that $\Delta t_j = E\{\Delta T_j\}$; i.e. the deterministic model only applies to mean time behavior. Even with the sample sizes employed, the $E\{\Delta T_j\}$ do not decrease in a smooth manner. Thus, there is a fog imposed by the finite sample size and the experimental technique through which we must examine results obtained in the data analysis, the smaller the sample size and the poorer the experimental technique the denser the fog.

Equation (16) is used to estimate the $\beta_j \bar{s}_o'$. In data sets b), c), and d), the estimates approximate a straight line except for the first few initial points; thus transient behavior is initially present before regular behavior is observed. We have already indicated that this transient behavior is most likely due to the small gradual rise in specimen temperature resulting from internal material hysteresis before a constant temperature slightly above the ambient air temperature is reached.

We also observe that the straight line character of the $\beta_j \bar{s}_o'$ estimates persists to the end of the crack length generated even though in some cases the final crack length is close to the specimen boundary. Thus, the effect of the boundary does not seem to be significant.

In all events, we find for each of the six data sets considered the straight line form

$$\beta_j \bar{s}_o' = \beta_o \bar{s}_o' (1 - c\bar{y}_j) \tag{47}$$

$$\beta_y \bar{s}_o' = \beta_o \bar{s}_o' (1 - cy) \tag{48}$$

where $\beta_o = \lambda_o/\upsilon kT$. With crack length as the only macro observable, we find there are three material parameters present, namely α or ΔG^+, β_o or λ_o/υ, and c. Zhurkov and Krausz-Eyring, employ only two constant material parameters in their model of time to failure under constant load, and static load data support their parameter assumptions. In some fatigue life models (no observable) [14,15], two constant material parameters also are employed. Further, the models of FCG presented in [11,12], where there is an observable, also assume two constant material parameters; however, these investigators did not perform the same type of evolutionary (y_i, t_j) data analysis as we employ, and thus it is not possible to determine if their parameters depend on y. In the model of FCG presented here, it is essential for evolutionary predictive accuracy that there be three material parameters. To see this, let us write ($\epsilon = 1$, $z = 1/4$, $h(\tau) = \sin \tau$)

$$u_j = \frac{2\beta_j \bar{s}_o'}{1 - .75\,\bar{y}_j} = \frac{2\beta_o \bar{s}_o' (1 - c\bar{y}_j)}{1 - .75\,\bar{y}_j}, \tag{49}$$

which is the only quantity involving the two material parameters β_o and c. If β_j does not depend of y, then

$$u_j = \frac{2\beta_o \bar{s}_o'}{1 - .75\,\bar{y}_j}. \tag{50}$$

Let us calculate Δt_j from (16) using these equations and the VHG Data. At $\bar{y}_j = .216535$ ($\bar{a}_j = 16.5$ mm.), let us fix the $\beta_o \bar{s}_o'$ in (50) so that the $(\Delta t_j)_2$ obtained using (16) is the same as the $(\Delta t_j)_1$ obtained using (49) in (16). Then, at $\bar{y}_j = .464878$ ($\bar{a}_j = 35.5$ mm.), we find that the ratio

$$\frac{(\Delta t_j)_1}{(\Delta t_j)_2} = 6.135490 \times 10^{-6} . \tag{51}$$

It follows that if we neglect the dependence of $\beta_j \bar{s}_o'$ on $\bar{y}_j$, as is done in (50), we will predict t_j that are much smaller than observed. Thus, we see that if only time to failure is of interest, then two constant material parameters appear to suffice, but if evolution of crack growth is of interest three constant material parameter must be used.

We know from Part I that a decrease in λ means an increase in material strength. Since from (37) $\lambda_y = \lambda_o(1 - cy)$, it is clear that the material is increasing in strength at a constant rate with respect to y, which implies the materials employed show work hardening. This implication is consistent with what is known about the behavior of such materials. What do we currently know about what β_o or λ_o and c are dependent upon?

First, let us note some information provided by other investigators. The data in [3] suggest that λ_o and c do not depend on T. Further, [16] suggests that λ_o and c depend on how the material is formed into components. We shall assume both hold. However, direct experimental evidence is needed to verify these assumptions.

β_o is related to λ_o through the second of (38); i.e. β_o depends on T although we are assuming λ_o does not. We shall confine attention to β_o in what follows.

The analysis of the GD Data shows, by means of (36) and Figure 4, that β_o depend on $\bar{s}_o'$ or $\bar{s}_o$ and Δs, assuming $\epsilon = 1$, $z = 1/4$, 1 $h(\tau) = \sin \tau$. Figures 5 and 6 and their ms. approximate straight lines reveal that β_o also depends on ϵ and z when $h(\tau) = \sin \tau$. Thus, given the data analyzed and the material employed, we know that β_o depends on $\bar{s}_o$, Δs, T, ϵ, and z when $h(\tau) = \sin \tau$. However, we do not have data with which to determine if β_o depends on the periodic wave form $h(\tau)$ for fixed $\bar{s}_o$, Δs, ϵ, z, and T.

Actually, in (42) we assume β_o depends on just $\bar{s}_o'$. This is a reasonable assumption since the dependence of β_o on $\Delta s'$, is relatively weak in comparison to its dependence on $\bar{s}_o'$ for Δs not small. Even so, the values of $\bar{s}_o'$ employed in (42), and by implication the values of $\bar{s}_o$ and Δs, should not be too far outside the range of values employed in the GD Data. Next, consider

what we have learned about c.

The adjacent table has been complied from results given in the previous section.

Table 1

Material	$\bar{s}_o'$	β_o	c
Al. alloy 2024-T3	8767	.00296039	.725106
Al. alloy 2024-T3	10820	.00246603	.723869
Al. alloy 7075-T6	10246	.00260708	.722287
Al. alloy 7075-T6	10004	.00269365	.727481
Al. alloy 7075-T6	6830	.00388267	.722104

The remarkable point suggested by this table is that irrespective of the aluminum alloy, specimen thickness, and the $\bar{s}_o'$ considered, c remains essentially the same with an average value .724051 and a maximum deviation of .47% for $\epsilon = 1$, $Z = 1/4$, different temperatures, and $h(\tau) = \sin \tau$. More data are needed to investigate this point.

We know from Figures 5 and 6 and the associated m.s. approximate straight lines that c depends on ϵ and z. Other conditions being the same, we have no data on how c might vary with $h(\tau)$. Thus, based on the specimen geometry and material considered, c depends on ϵ and z and possibly $h(\tau)$, but does not depend on $\bar{s}_o'$ and T. These observations have implication concerning the amount of testing required for accurate prediction.

Accurate evolutionary prediction under different load conditions and temperature requires that we have accurate estimates of β_o and c as a function of $\bar{s}_o'$ for a given component geometry, T, ϵ, z, and wave form $h(\tau)$, and assuming no transient material behavior. If we have three reasonably high replication sets of FCG tests with the $\bar{s}_o'$ substantially different but with the other quantities fixed, we can estimate β_o or λ_o and c for each test $\bar{s}_o'$. We plot β_o or λ_o and c against $\bar{s}_o'$ and put a smooth curve through these points. At any other $\bar{s}_o'$ (not too far out of the range of the test values), we can obtain appropriate values for β_o or λ_o and c. Then, employing (16), we can predict mean t_j for this $\bar{s}_o'$ and T if different from the test values. While these tests

are not likely required for obtaining c, we know they are for estimating β_o or λ_o, assuming λ_o and c do not depend on T.

Equation (44) merits a few comments. First, as must be the case, we obtain this equation when using the other two wave forms provided we correct the right based side of (18) and of (19) so that $\Delta s \geq 0$ can be small. Second, let us rewrite (44) as

$$\frac{\Delta y_j}{\Delta t_j} = \alpha z \bar{y}_j e^{\frac{r_\sigma \beta_o \bar{s}_o' (1-c\bar{y}_j)}{1-(1-\epsilon z)\bar{y}_j}}, \tag{44'}$$

We can now compare (44') with (3) and (10) in [13], on taking into account differences in notation. We observe in this static load case the results differ because we are following the evolution of an observable with a nonuniform stress distribution and they do not do this.

Let us rewrite (19) as

$$\frac{\Delta t_j}{2} = \frac{\Delta y_j}{\alpha z \bar{y}_j} e^{-\frac{r_\sigma \beta_j \bar{s}_o'}{1-(1-\epsilon z)\bar{y}_j}}, \tag{19'}$$

which is the same form as (44), except for a factor two, even though in (19) we have a periodic load and Δs is not small. It is clear that when $h(\tau)$ has a rectangular wave form and $\bar{s}_o = \bar{s}_o'$, the static load produces the same evolutionary result in half the time provided the β_j remain the same. This possibility was noted by Regel and Leksovsky [15] although their approach to the fatigue problem is very different from ours but similar to that employed in [14].

Finally, we note that it is possible to use the deterministic model for accelerated testing in useful ways. One way to accelerate a test is to either increase $\bar{s}_o$, or Δs, or both by constant amounts over the condition at which a prediction is required. We next estimate β_o and c at the accelerated test condition. If we assume these estimates will apply at the $\bar{s}_o$ and Δs for which prediction is required, then we can employ them to produce the predicted behavior. However, we know that β_o depends on $\bar{s}_o$ and Δs; i.e. the load interaction will be different at the two load conditions. The same problem was noted in [20]. Hence, the accuracy of the predicted behavior

is open to question when $\bar{s}_0$ and Δs are changed to accelerate the test. However, since α and β depend on T in a known manner, another way to accelerate a test is to increase T. The second way has some advantages.

We already know from Figure 7 and from [3, 16] that a small change in T produces a significant change in mean life behavior. Suppose we want to predict mean life behavior at $T_0 = 302^\circ K$ with specified $\bar{s}_0$, Δs, ϵ, z, and $h(\tau) = \sin \tau$. Let us test at $T_2 = 312^\circ K$ with the same specified quantities. Figure 7 indicates that the time of specimen testing is reduced by a factor of about 3. If we test instead at $T_3 = 322^\circ K$, the time the specimens are under load is reduced by a factor of about 10. This method of accelerating testing has the advantage of eliminating questions that may arise concerning the effect on mean life behavior due to load interaction when changing $\bar{s}_0$ and Δs with T held constant. The second way of accelerating a test thus has advantages over the first way.

5. Probabilistic Model

The model discussed so far is deterministic. However, the FCG phenomena is statistical. Even with controlled temperature T, load F(t), and humidity, as in the VHG-experiments, variability among the results for different test specimens is significant; the variability in this case is primarily due to variability in material behavior. A second and different source of variability in FCG is the variability always present in the load, temperature, and environment; i.e. in experimental technique. These are the sources of the statistical nature of the FCG phenomenon. Inspection of the sample function graphs of the data sets of crack growth in [17] indicates that the VHG Data has the least scatter. This implies that the noise due to experimental technique is least for these data. Thus, we expect the least scatter in the moment estimates and edf's (empirical distribution functions) of the ΔT_j and Q_j (see below) in the VHG Data, and this is the case. In this paper, we employ an elementary approach in our first attempt to model material variability.

Consider (16):

$$\Delta t_j = E\{\Delta T_j\} = \frac{\Delta y_j \sqrt{2\pi}}{\alpha z y_j} \sqrt{u_j \Delta s'}\, e^{-u_j}, \tag{52}$$

where we specifically note $h(\tau) = \sin \tau$, Δs is not small, and

$$\alpha = \frac{kT}{h} e^{-\frac{\Delta G^+}{kT}},$$

$$u_j = \frac{\beta_j (1 + \epsilon)\bar{s}_o'}{1 - (1 - \epsilon\, z)\bar{y}_j},$$

$$\beta_j = \frac{\lambda_j / \upsilon}{kT},$$

We assume $\bar{s}_o$, Δs, T, and the environment are controlled to be constant. We have already assumed in these equations that the mean bond force f is specified by the deterministic expression $f = s(t, \xi)/\upsilon$. Thus, the only sources of material variability lie in ΔG^+ and $\beta_j \bar{s}_o'$.

ΔG^{+} is a free energy, for such a thermodynamic quantity, the variability is small so that in this initial stage of modeling variability we will neglect it even though α is sensitive to changes in ΔG^{+}. Thus, $\beta_j \bar{s}_o{}'$ is the only source of variability that we will consider at this time.

Let

$$z_j = \sqrt{u_j \Delta s'}\, e^{-u_j} ; \tag{53}$$

it follows from (52) that

$$\Delta t_j = E\{\Delta T_j\} = \frac{\Delta y_j \sqrt{2\pi}}{\alpha Z \bar{y}_j} z_j . \tag{54}$$

Next, let

$$\Delta T_j = \frac{\Delta y_i \sqrt{2\pi}}{\alpha z \bar{y}_j} Z_j ,$$

where $Z_j = (1 + P_j) z_j$ and $E\{P_j\} = 0$. Then, from (54),

$$E\{\Delta T_j\} = \frac{\Delta y_j \sqrt{2\pi}}{\alpha z \bar{y}_j} z_j ,$$

which is (52).

Now let U_j and Q_j be two additional rvs with

$$U_j = u_j(1 + Q_j) ,$$

and let

$$Z_j = \sqrt{U_j \Delta s'}\, e^{-U_j} = \sqrt{u_j(1 + Q_j)\Delta s'}\, e^{-u_j(1 + Q_j)} \tag{55}$$

We now have

$$E\left\{\sqrt{U_j \Delta s'}\, e^{-U_j}\right\} = z_j \ ,$$

$$E\left\{\sqrt{u_j(1+Q_j)\Delta s'}\, e^{-u_j(1+Q_j)}\right\} = z_j \ ,$$

and hence it follows that

$$E\left\{(1+Q_j)^{1/2}\, e^{-u_j Q_j}\right\} = 1 \ . \tag{56}$$

The quantity u_j is of the order of 50 for Al.. This means that the Q_j are small. Then with

$$\log Z_j/z_j = \frac{1}{2}\log(1+Q_j) - u_j Q_j$$

$$\simeq -(u_j - \frac{1}{2})Q_j \ ,$$

it follows that

$$Z_j/z_j \simeq e^{-(u_j-\frac{1}{2})Q_j} \ ,$$

$$Q_j \simeq -\frac{\log Z_j/z_j}{u_j - \frac{1}{2}} \tag{57}$$

At the sample function level

$$q_{j,n} \simeq -\frac{\log z_{j,n}/z_j}{u_j - \frac{1}{2}} \tag{58}$$

where

$$z_{j,n}/z_j = \frac{\Delta t_{j,n}}{E\{\Delta T_j\}} \tag{59}$$

Further,

$$P\left\{Q_j \le q_j\right\} = P\left\{-\frac{\log Z_j/z_j}{u_j - \frac{1}{2}} \le q_j\right\},$$

$$= P\left\{Z_j/z_j \ge e^{-(u_j-\frac{1}{2})q_j}\right\}, \text{ or}$$

$$F_{Q_j}(q_j) = 1 - F_{Z_j/z_j}\left\{e^{-(u_j-\frac{1}{2})q_j}\right\} \tag{60}$$

This method of introducing the Q_j avoids addressing the joint problems of how to assign variability at the micro material level, and how to convert such a variability into macro stochastic FCG equations in a physically satisfactory manner. We defer addressing these two problems at present, and go on to determine what a data analysis says about the statistical properties of the Q_j. We first consider the VHG Data which has the highest replication number (sixty-eight) and the variability at the sample level is small. We assume $\epsilon = 1$, $z = 1/4$, and $h(\tau) = \sin \tau$.

First, consider the four crack length intervals of different lengths centered as closely as the data permits on the crack length 26 mm:

(25.8 mm., 26.2 mm.), (25.6 mm., 26.6 mm.), (25 mm., 27 mm.), and (24.6 mm., 27.6 mm.) ; (61)

The crack lengths of these intervals are respectively. .4 mm., 1 mm., 2 mm., and 3 mm.. We find from the data in each case the sample times $\Delta t_{j,n}$ required to cross these intervals, where $n = 1, \cdots, 68$ and $j = 1, \cdots, 4$ refers to the above intervals. We next estimate the $E\{\Delta T_j\}$ and compute the sample $q_{j,n}$ from (58). The estimated moments of the Q_j are given in

Table 2

j	m_Q	σ_Q^2	m_Q/σ_Q	$\gamma_{1,j}$
1	256.265×10^{-6}	9.324534×10^{-6}	.083922	-.45514
2	168.294×10^{-6}	6.099563×10^{-6}	.068143	-.355644
3	123.985×10^{-6}	4.521016×10^{-6}	.058313	-.631304
4	98.6324×10^{-6}	3.535632×10^{-6}	.052455	-.909978

The smoothed edf's of the standardized variable $\overline{q}_{j,n} = (q_{j,n} - m_j)/\sigma_j$ are plotted in Figure 8. These smoothed edf's are obtained from the smoothed edf's of the ΔT_j employing (60). The $q_{j,n}$ range from approximately -8×10^{-3} to 7×10^{-3}.

The means are small and decrease as the crack length interval increases. The variances decrease as the crack length interval increases. These results, particularly the last, suggest that the Q_j are the result of some type of smoothing operation over increasing crack lengths at the micro level.

The skewness coefficients $\gamma_{1,j}$ are all negative with average; -.588110 and not close to zero. This results indicates that the Q_j are not normal random variables.

That the smoothed edf's are close is not surprising in view of the fact that this is the case for the smoothed edf's of the Δt_j (see [16]).

Next consider the four crack length intervals

(21 mm., 22 mm.), (26 mm., 27 mm.), (31 mm., 32 mm.), and (36 mm., 37 mm.) , (62)

each having Δa_j = 1 mm.. The estimated moments of these Q_j are given in

Table 3

j	m_Q	σ_Q^2	m_Q/σ_Q	$\gamma_{1,j}$
1	189.706×10^{-6}	6.200268×10^{-6}	.076186	-.07860
2	89.9706×10^{-6}	5.088137×10^{-6}	.038556	-.372504
3	190.265×10^{-6}	7.719240×10^{-6}	.068481	-.547555
4	181.074×10^{-6}	9.981985×10^{-6}	.057312	-.284855

The correlation coefficients ρ_{jk} are estimated and given in

Table 4

$$\rho_{jk} = \begin{cases} \begin{matrix} j, j+1 & j, j+2 & j, j+3 \end{matrix} \\ .154233 \\ & .132162 \\ & & .370998 \\ .173791 \\ & .240113 \\ .470985 \end{cases}$$

The smoothed edf's of the standardized $\bar{q}_{j,n}$ are shown in Figure 9, with the same approximate range for the $q_{j,n}$ as in the previous case.

The estimated means, variances, and skewness coefficients fluctuate about a constant values; the averages of these estimates are 162.004×10^{-6}, $7.247\ 408 \times 10^{-6}$, and -.320879, respectively. Again the nonzero skewness coefficients, which are negative, indicates that these Q_j are also not normal random variables. The correlation coefficients are all positive; thus, the Q_j are statistically dependent. The smoothed edf's of the standardized random variables are also close to one another and the set of edf's in Figure 8 is close to the set in Figure 9. These results are for one $\bar{s}_o$ and Δs with different crack length intervals.

Next, let us consider the GD Data where there are three load conditions ($\bar{s}_o$, Δs), and there are sixty replications for each condition. We consider three crack length intervals:

(16 mm. – 17 mm.), (17 mm. – 18 mm.), (16 mm – 18 mm.)

The results presented here are for different loads but for each of the indicated crack length intervals.

Figures 10, 11, 12 display the edf's of the standardized Q's for the three load conditions at the indicated crack length intervals. These edf's are obtained from the edf's of the ΔT_j by employing (55) and (60). We see from the figures that the edf's of the standardized Q_j are close to one another for different $\bar{s}_o$ and Δs. However, we see from Tables 5, 6, and 7 that some of the γ's are positive; this is likely due either to sample size variability or to variability in the experimental program or to both, and occurs when the positive γ_1's of the ΔT_j are much less than one.

Tables 5, 6, and 7 also give estimated moment results for Q's at the same crack length intervals. We observe that the moments of the Q's not only depend on the crack length interval but also on the load. The Q's for the intervals (16 mm., 17 mm.) and (17 mm., 18 mm.) are correlated as is the case for all non-overlapping intervals, which is not surprising since we already know the ΔT_j on non-overlapping intervals are positively correlated. We observe from these tables that the mean m_Q, the variance σ_Q^2, and the signal to noise ratio m_Q/σ_Q increase in all cases as $\bar{s}_o'$ decreases. However, since the $\bar{s}_o'$ are not well spaced, we cannot form a firm idea of how these quantities depend on $\bar{s}_o'$; this point must be taken up at a later time when data are available at more than three points or when there is better spacing in the $\bar{s}_o'$ values.

Table 5

Q, (16 mm., 17 mm.)

	m_Q	σ_Q^2	m_Q/σ_Q	γ_1	$\bar{s}_o'$
S1	$.292595 \times 10^{-3}$	$.108816 \times 10^{-4}$	.0886993	-.294657	10246
S2	$.398630 \times 10^{-3}$	$.146009 \times 10^{-4}$	.104323	-.430016	10004
S3	$.984548 \times 10^{-3}$	$.374576 \times 10^{-4}$	.160867	-.0755493	6830

Table 6

Q, (17 mm., 18 mm.)

	m_Q	σ_Q^2	m_Q/σ_Q	γ_1	$\bar{s}_o'$
S1	$.222031 \times 10^{-3}$	$.851427 \times 10^{-5}$	.0760923	.210108	10246
S2	$.363674 \times 10^{-3}$	$.135120 \times 10^{-4}$	.0989356	-.249759	10004
S3	$.942224 \times 10^{-3}$	$.383306 \times 10^{-4}$	.156321	.00992309	6830

Table 7

Q, (16 mm. - 18 mm.)

	m_Q	σ_Q^2	m_Q/σ_Q	γ_1	$\bar{s}_o'$
S1	$.229298 \times 10^{-3}$	$.876723 \times 10^{-5}$	.0776100	.111876	10246
S2	$.356154 \times 10^{-3}$	$.130594 \times 10^{-4}$	.098554	-.426007	10004
S3	$.880428 \times 10^{-3}$	$.340063 \times 10^{-4}$	.150975	.0728710	6830

6. Discussion of Probabilistic Model

We have introduced randomness into the macro deterministic difference form (16) of the FCG process by the expedient of assuming the growth control parameter is multiplied by a random factor. We have already commented on the fact that this method of introducing the ever present variability may have short-comings when the physics of the random micro material behavior is the starting point for introducing randomness. The behavior of mean and variance of the Q_j, when the crack length intervals (61) are employed in the VHG Data, suggests that these Q_j are the result of the some smoothing operation at the micro level over the intervals, which indicates the micro starting point merits attention. Further investigation on this approach is required.

The closeness of the smoothed edf's of standardized Q's in Figures 8 and 9 for different crack length intervals but the same $\overline{s}_o$ and Δs is similar to what was reported earlier [17, 18] for the ΔN_j (ΔT_j in present paper). What is of interest is that the edf's of the standardized Q_j are close to one another for the same crack length interval but with different $\overline{s}_o$ and Δs, as is clear from Figures 10, 11 and 12 obtained from the GD Data; further, if one compares the results in this set of figures, we observe that these edf's are close to one another even though the crack length intervals are different. All of this suggests that the standardized Q_j appear to be the same, having a negative skewness, in spite of the fact we are viewing them through the fog imposed by the finite sample size and experimental variability.

The correlation coefficients in Table 4 are not large but are positive. Since the intervals in (62) are well separated, this results is not surprising, especially in view of the results on the correlation coefficients of the ΔN_j given in Table 3 of [17] and first reported and modeled by us in [18]. Thus, the statistical dependence of the Q_j is to be expected. This means, of course, that the Q_j form a family of dependent random variables indexed on the interval Δy_j; i.e. they constitute a random function.

The non normal character of the Q_j can be explained as follows: in virture of the fact that

$$(1 + Q_j)u_j = \frac{(1 + \in)(1 + Q_j)\beta_j \bar{s}_o'}{1 - (1 - \in z)\bar{y}_j},$$

we observe that the $(1 + Q_j)\beta_j \bar{s}_o'$ represent the random nature of the dimensionless work done in breaking a bond. Since this work depends on the variability inherent in the bond force f and in the distance λ a bond is extended in breaking, the variability in the work done in breaking a bond is dependent on the joint distribution of these two random elements. Thus, the non normal character of the Q_j is not unexpected. We also note that the negative skewness of the Q_j or $1 + Q_j$ suggests the possibility that the origin of these rv's might be associated with a "weakest link" concept. In the present context, this suggest that the underlying bond breaking process might be associated with (governed by) a mechanism based on steps determined by the least work in the breaking process.

It is clear from (60) that the distributions of the Q_j depend on the u_j. We know the u_j depend on $\in$, z, T, $\bar{s}_o'$ or $\bar{s}_o$ and Δs, and $h(\tau)$. It follows that the distributions of the Q_j depend on the same quantities. Thus, it is possible to study how changes in these quantities influence the distributions of the Q_j. However, we will not attempt a study of this point in this paper..

There are a number of additional parameters that must be estimated if the model is to account for the random nature of the Q_j or Z_j. It appears that the same high replication tests needed to estimate the material parameters in the deterministic model will suffice to supply estimates for these additional parameters. Thus, the same set of tests, at the same $\in$, z, and $h(\tau)$, is all that is needed to render the model a predictive tool whether or not randomness is included.

Finally, we mention that [22] contains some of our initial thoughts on how reaction rate theory might be applied to the FCG problem.

7. Conclusion

We present a deterministic macro model of FCG based upon a micro result provided by reaction rate theory. A center crack panel under periodic tensile load is the basic physical situation considered. The model contains explicitly the stress distribution $s(t,\xi)$ on the unbroken portion of the crack plane, the far field stress $s_o(t)$, the absolute temperature T, and two material parameters ΔG^+ and β of which ΔG^+ can be estimated from available information, but the growth control parameter β must be estimated from test data since it depends on how the material is formed into specimens/components and the environment.

For a reasonable choice of $s(t,\xi)$ that assumes no dynamical effects present in the specimen/component, we find an evolutionary equation in the dimensionless crack length y and two other quantities δ and r_σ that describe aspects of the evolution of the stress distribution Joint evolutionary equations for these quantities are needed to determine y, δ, and r_σ as functions of time, and to determine if they form a state vector. We conclude from this approach that the FCG process is more complex than can be described by y alone.

At the present time, no such joint evolutionary equations are available. To proceed with a study of some of the capabilities of the model based upon a statistical analysis of currently available data, we introduce constraint equations for δ and r_σ that reflect general properties of polycrystaline ductile metals in fatigue, and use the resulting deterministic constrained equation to describe the evolution of y, containing the two constraint parameters ϵ and z in addition to ΔG^+, β, T, and the far field tensile load $s_o(t) = \bar{s}_o + \Delta s\, h(wt)$, where $h(\tau)$ is the periodic wave form. An equation of this type only can apply to the mean behavior of the crack growth.

Available reasonably high replication FCG data are for simple harmonic tensile load variation and specimens of polycrystaline ductile metals. For a load of this type, the constrained equation for the evolution of y can be useful approximated by a difference equation in discrete time and discrete crack length that not only makes parameter estimation of β straight forward, but also permits us to study the effect of changes in T, $h(\tau)$, $\bar{s}_o$, Δs, and β on the FCG process.

We conclude from a parameter estimation study based upon these data and the mean model that

a) there can be transient behavior in the $\beta_j \bar{s}_o{}'$ estimates due to a temperature change or a load change,

b) the growth control parameter β_y depends on the crack length through the relation $\beta_y = \beta_o(1-cy)$ once the transient effect of the initial temperature change ceases,

c) there are three material parameters ΔG^+, β_o, and c when there is only one observable y and a fixed set of constraint parameters $\in$ and z,

d) the relation $\beta_y = \beta_o(1-cy)$ is due to the work hardening properties of the material,

e) β_o depends on $\bar{s}_o$ and Δs but c does not appear to do so, both depend on $\in$ and z, β_o depends on T but λ_o and c do not appear to do so, β_o and c may depend on $h(\tau)$, and

f) two or three suitable tests are needed to estimate β_o and c so that the model can predict crack growth behavior over a reasonable range of $\bar{s}_o$ and Δs values.

Further, we conclude from e) that when $s_o(t)$ is oscillatory but not periodic, transient material behavior may occur.

The constrained model or difference equation in Δy_j and Δt_j contains explicitly the wave form $h(\tau)$, T, $\bar{s}_o{}'$ and Δs. We conclude that predicted Δt_j for a given Δy_j is sensitive to changes T, $\bar{s}_o{}'$ and Δs, and the predicted Δt_j can change substantially for changes in $h(\tau)$ with the same $\bar{s}_o{}'$, Δs, and T. Thus, we conclude that when conducting experiments and when predicting crack growth in service these quantities, particularly T and $h(\tau)$, play a significant role.

The possibility of increasing only T to accelerate a test is a useful observation since such a procedure appears to eliminate load interaction problems that may arise when $\bar{s}_0$ or Δs are changed with T constant, as is usually done. In addition, we note that this method of

accelerating a test can be used with profit when conducting the two or three tests needed to determine how β_o and possibly c depend on the load which, as we have remarked above, are needed to predict life under different $\bar{s}_o'$ and Δs than employed in these tests. We conclude that the explicit presence of T in the model is an important feature of this model.

The constrained model with one observable y contains explicitly the far field stress variation $s_o(t)$. Thus, by means of numerical integration, we can predict crack growth behavior for any tensile $s_o(t)$, including static load. However, we conclude from a) and e) above that transient material behavior may put accurate prediction based on this model into question when $s_o(t)$ is oscillatory but not periodic. We conclude that for accurate prediction for any oscillatory non periodic $s_o(t)$ it may be necessary to have the joint evolutionary equations for y, δ, and r_σ for it is only by such a model that we may be able to take into account the load history dependence of the material.

The unit-jump B-model [19] contains the probability transition matrix P with elements p_j, q_j, $(p_j + q_j = 1)$ on the jth line. Since $(b_j - b_{j-1})/q_j = E\{\Delta T_j\}$, we conclude that it is now possible relate the $(b_j - b_{j-1})/q_j$ to T, $\bar{s}_o'$, Δs, and $h(\tau)$. This is an important point.

The model assumes that the rate of single bond breaking κ_b is determined by a single energy barrier and there is no bond healing. It is clear that it is possible to relax our assumptions in order to accommodate other possibilities. We conclude that the simple model presented here permits extension in a number of directions of this type. Bond healing can be accommodated in B-models by assuming nonzero elements below the main diagonal in P.

The specimen geometry and loading can be changed. A new model would have to be created for each new situation. This constitutes another area into which this type of model can be extended.

If there are dynamical effects in the specimen, $s(t,\xi)$ cannot have the simple form we have assumed. It may be possible to include this feature although we have not considered it.

Variability in material behavior is introduced into the deterministic difference equations by the simple expedient of multiplying the growth control parameter β_j by $(1 + Q_j)$, where the

Q_j are a family of random variables indexed on (y_{j-1}, y_j); Δt_j is then replaced by the random variable ΔT_j. We already know from previous work [17,18] and also from the statistical analysis conducted here that the ΔT_j are dependent and non-normal with positive skewness. We conclude from the analysis of the VHG and GD Data presented above that the Q_j are dependent and non normal with negative skewness. We also conclude that the distribution of the Q_j and their moments depend on $\bar{s}_o{}'$, Δs, and T for given ε and z, although given the database it is not possible at this time to determine the nature of this dependence on $\bar{s}_o{}'$ and Δs. For the same reason, we can not determine the nature of this dependence on $h(\tau)$.

The closeness of the standardized edf's of the Δt_j and of the Q_j requires explanation, since it suggests that there is an underlying random material process present. It is possible, as mentioned earlier, that if we introduce material randomness at the micro level and develop a stochastic macro model from this starting point. We can find an explanation for this interesting experimental fact.

Parameter estimation for the above stochastic model can be handled from data needed to estimate the parameters of the deterministic model.

Based upon the above, we conclude that the model appears capable of illuminating many of the complexities that are experimentally observed in the FCG process, it has useful predictive possibilities, and it suggests a simple method for accelerating FCG tests.

References

1. Kozin F., and Bogdanoff J.L., "Cumulative Damage Model for Mean Fatigue Crack Growth Based on the Kinetic Theory of Thermally Activated Fracture," Energy Fract. Mech., to appear.

2. Handbook of Mathematical Functions, Ed. by Abramowitz M. and Stegun I.A., Dover, 9th Printing, 1970, p. 377.

3. Zhurkov S.N., "Kinetic Concept of the Strength of Solids," Inter. Jour. Fract. Mech., Vol. 1, 1969, pp. 311-323.

4. Hudak S.J., "Development of Standard Methods of Testing and Analyzing Fatigue Crack Growth Data," AFML TR-78-40, 1978.

5. Virkler D.A., Hillberry B.M. and Goel P.K., "The Statistical Nature of Fatigue Crack Growth," AFFDL TR-78-43, 1978.

6. Ichikawa M., Hamaguchi M., and Nakamura T., "Statistical Characteristics of M and C in Fatigue Crack Propagation," Journ. of Int. Soc. of Materials Science Vol. 33, No. 364, Jan. 1984, pp. 8-13.

7. Ghonem H. and Dore S., "Experimental Study of the Constant Probability Crack Growth Curves under Constant Amplitude Loading," Engrg. Fract. Mech. Vol. 27, No. 1, 1987, pp. 1-25.

8. Krausz A.S. and Eyring H., "Deformation Kinetics," John Wiley and Sons, New York, 1975

9. Kozin F and Bogdanoff J.L., "On Life Behavior under Spectrum Loading," Engrg. Fract. Mech. Vol. 18, No. 2, pp. 271-283, 1983.

10. Yokobori T., "Strength, Fracture and Fatigue of Materials," P. Noardhoff, Groningere, The Netherlands, 1964.

11. Yokobori T., "A Kinetic Approach to Fatigue Crack Propagation," The Orowan Anniversary Volume, M.I.T. Press, pp. 327-338, 1969.

12. Krausz A.S. and Krausz K., "Fracture Kinetics of Crack Growth," Kluwer Academic Press, Boston, 1988.

13. Henderson, C.B., Graham P.H. and Robinson C.N., "A Comparison of Reaction Rate Models for the Fracture of Solids," Inter. Journ. of Fract. Mech., Vol. 6, No. 1, 1970, pp 33-40.

14. McKenna G.B. and Penn R.W., "Time-dependent Failure in Poly(methylmethacrylate) and Polyethylene," Polymer, Vol. 21, 1980, pp. 213-220.

15. Regel V.R. and Leksovsky A.M., "A Study of Fatigue within the Framework of the Kinetic Concept of Fracture," Inter. Journ. of Fract. Mech., Vol. 3, 1967, pp. 99-109.

16. Regel V.R., Slutsker A.I., and Tomashevskii E.E., "The Kinetic Nature of the Strength of Solids," Soviet Physics Uspekhi, Vol. 15, 1972, pp. 45-65.

17. Kozin F. and Bogdanoff J.L., "Probabilistic Models of Fatigue Crack Growth: Results and Speculation," Nuc. Energy & Design, Vol. 115, 1989, pp. 113-171.

18. Kozin F. and Bogdanoff J.L., "Probabilistic Models of Fatigue Crack Growth" II, Engrg. Fract. Mech., Vol. 20, 1984, pp 255-270.

19. Bogdanoff J.L. and Kozin F., "Probabilistic Models of Cumulative Damage," John Wiley & Sons, N.Y., 1985.

20. Kozin F. and Bogdanoff J. L., "An Approach to Accelerated Testing," Canadian Aeronautics and Space Journal," Vol. 29, No. 1, pp. 60-76, 1983.

21. Kozin, F. and Bogdanoff, J.L., "Role of Third Order Statistics in Discriminating among Models of Fatigue Crack Growth in Metals," Metallurgical Trans. A., Vol. 18A, Nov. 1987, pp. 1855-1859.

22. Bogdanoff J. L. and Kozin F., "Application of Physical Laws to Parametric Estimation for Probabilistic Models of Cumulative Damage," ICOSSAR89, San Franciso, Aug. 1989.

Figure Captions

Figure 1: E24.04.01 Round Robin Data. Estimates of $\beta_j \bar{s}_0'$ vs. crack length a. $a = 2.55$ y, $\epsilon = 1$, $z = 0.25$

Figure 2: GD Data. Estimates of $\beta_j \bar{s}_0'$ vs. crack length a. $h(\tau) = \sin \tau$, 21 points, $a = 50.8$ y, $\epsilon = 1$, $z = 0.25$.

Figure 3: GD Data. Estimates of β_0 vs. $\bar{s}_0'$. $h(\tau) = \sin \tau$, $\epsilon = 1$, $z = 0.25$.

Figure 4: IHN Data. Estimates of $\beta_j \bar{s}_0'$ vs. crack length a_x for variable ϵ and fixed $z = 0.25$. $h(\tau) = \sin \tau$, $a = 35$ y.

Figure 5: IHN Data. Estimates of $\beta_j \bar{s}_0'$ vs. crack length a for variable δ and fixed $\epsilon = 1.0$. $h(\tau) = \sin \tau$, $a = 35$ y.

Figure 6: VHG Data. Effect of changing T on a vs. t curve. $h(\tau) = \sin \tau$, $a = 76.2$ y, $\epsilon = 1$, $z = 0.25$.

Figure 7: VHG Data. Effect of changing $h(\tau)$ on a vs. t curve. $a = 76.2$ y, $\epsilon = 1$, $z = 0.25$.

Figure 8: VHG Data. Smoothed edf's of standardized q_j for variable Δa and fixed load. $h(\tau) = \sin \tau$, $a = 76.2$ y, $\epsilon = 1$, $z = 0.25$.

Figure 9: VHG DATA. Smoothed edf's of standardized q_j for fixed Δa and fixed load. $h(\tau) = \sin \tau$, $a = 76.2$ y, $\epsilon = 1$, $z = 0.25$.

Figure 10: GD Data. Edf's of standardized q_j for fixed Δa and variable load. $h(\tau) = \sin \tau$, $\epsilon = 1$, $z = 0.25$, $16 - 17$ mm.

Figure 11: GD Data. Edf's of standardized q_j for fixed Δa and variable load. $h(\tau) = \sin \tau$, $\epsilon = 1$, $z = 0.25$, $17 - 18$ mm.

Figure 12: GD Data. Edf's of standardized q_j for fixed Δa and variable load. $h(\tau) = \sin \tau$, $\epsilon = 1$, $z = 0.25$, $16 - 18$mm.

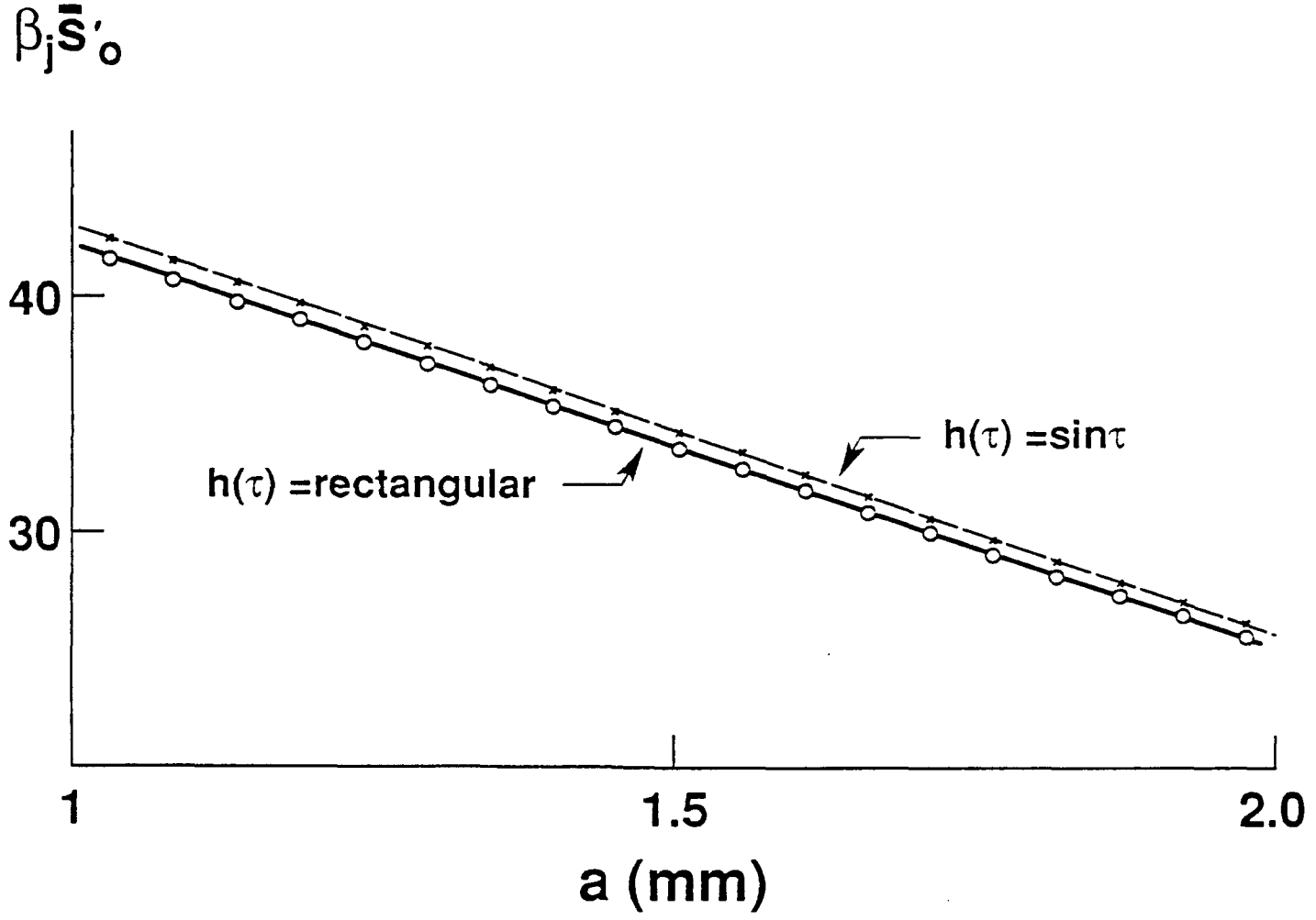

Fig. 1

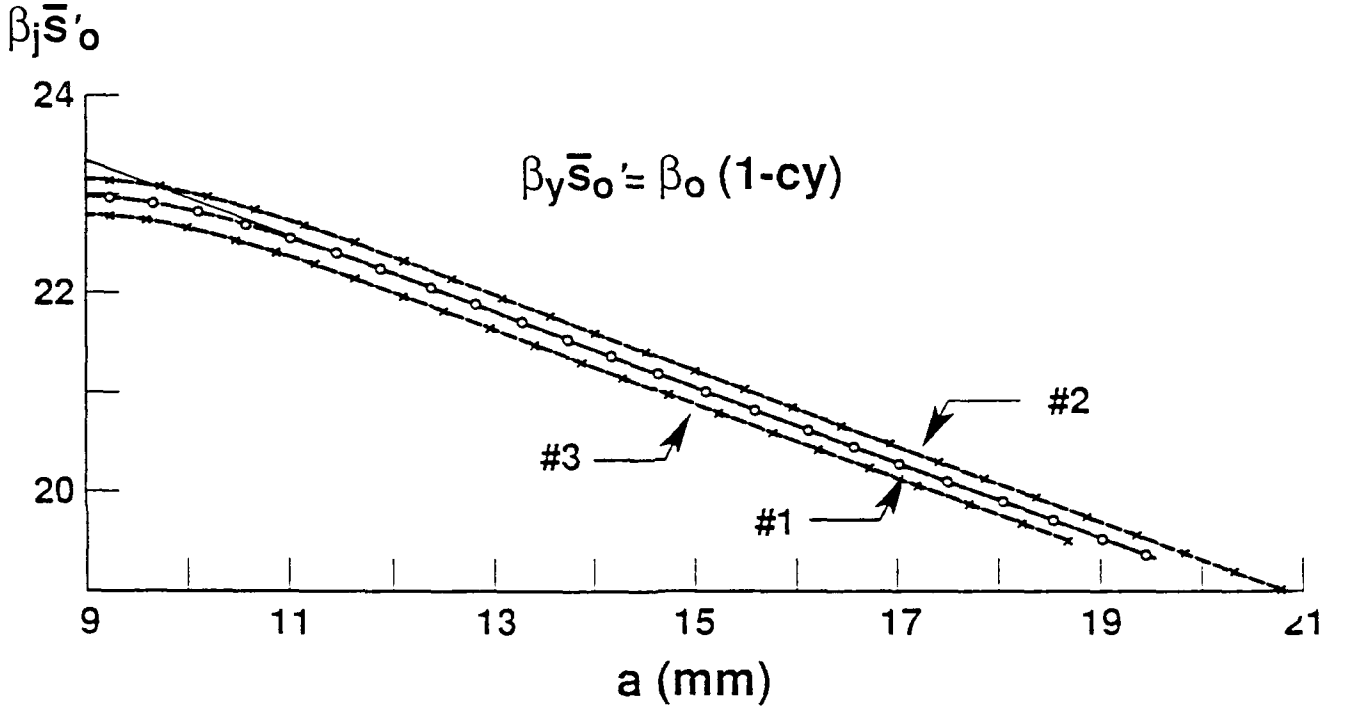
$\beta_j \bar{s}'_o$
24
22
20
$\beta_y \bar{s}_o' \cong \beta_o (1\text{-}cy)$
#2
#3
#1
9
11
13
15
17
19
21
a (mm)

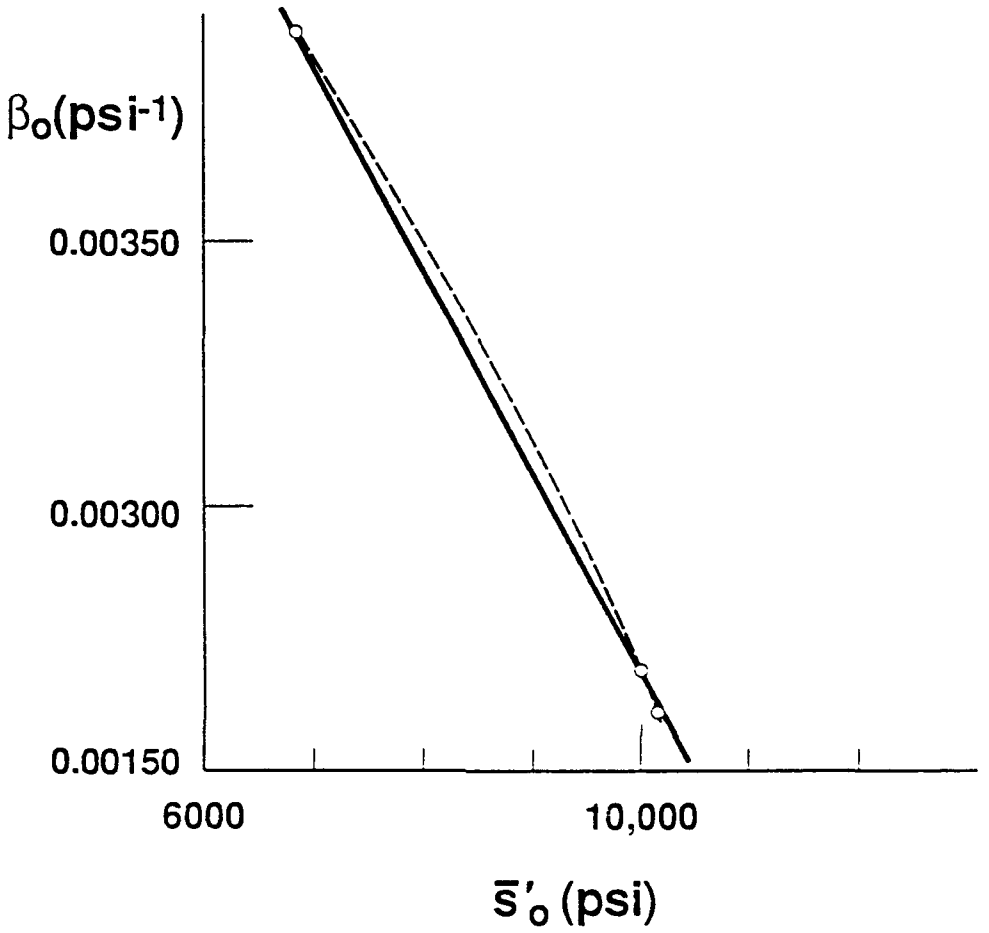

Fig 3

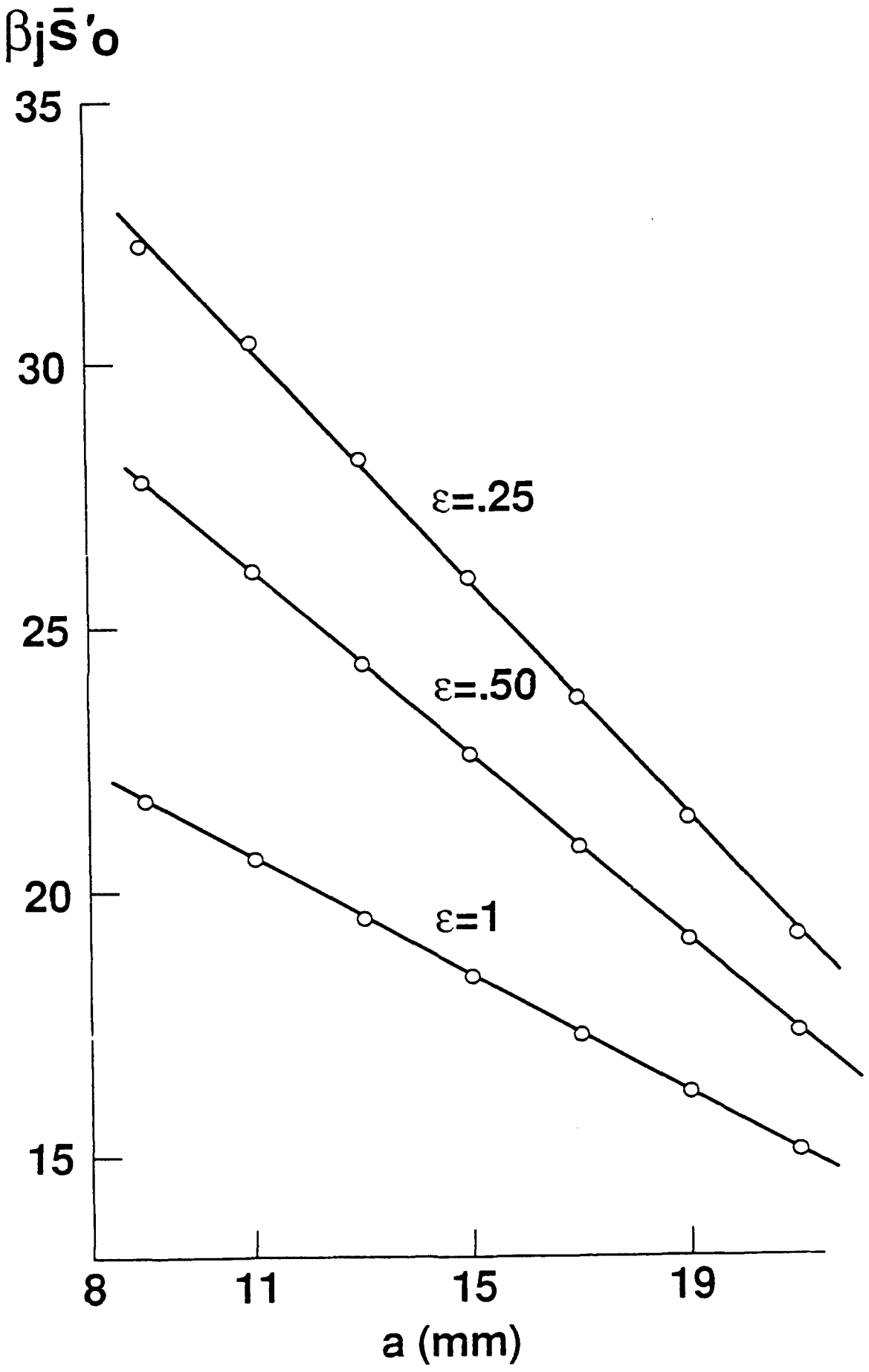

FIG. 4

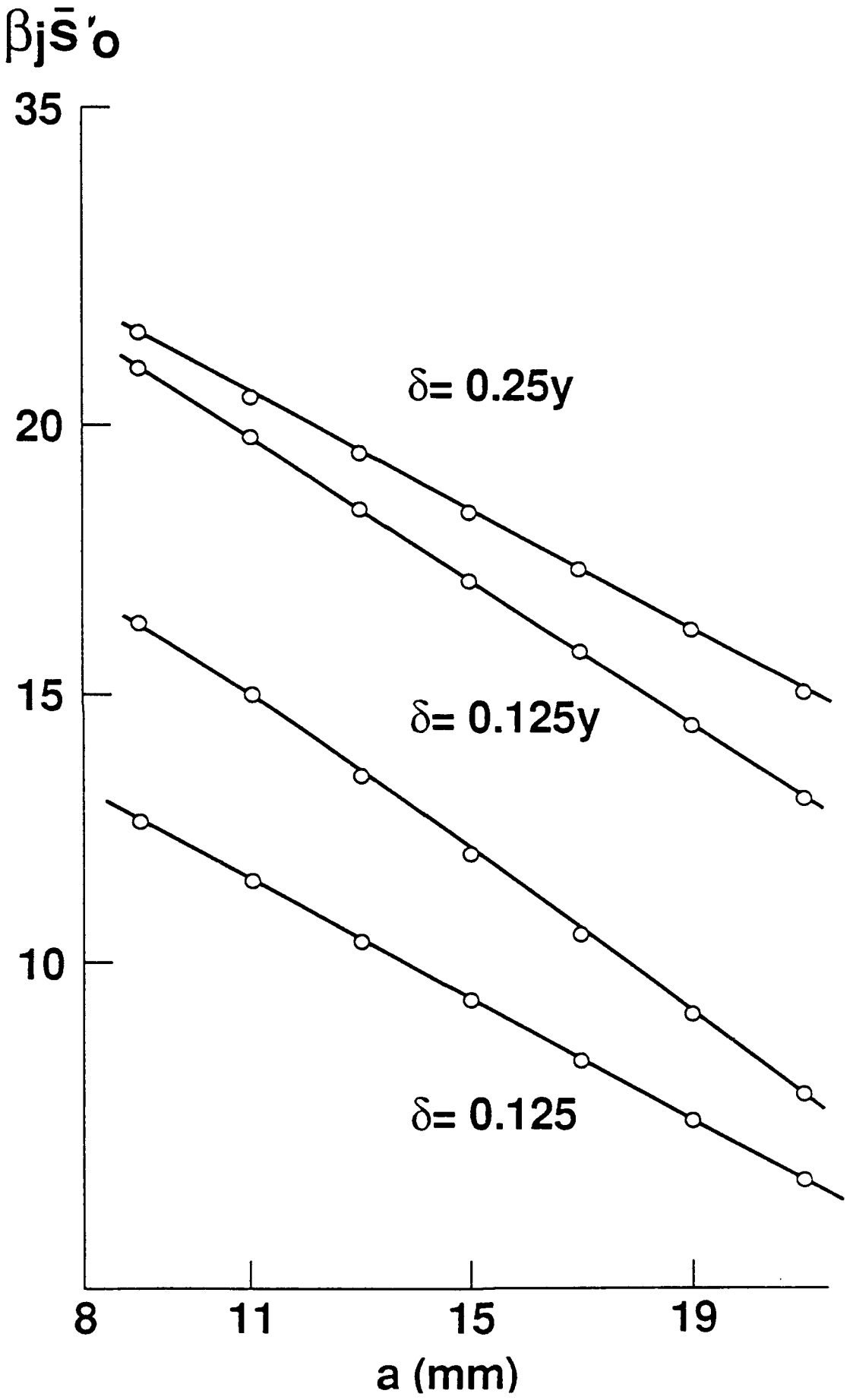

FIG 5

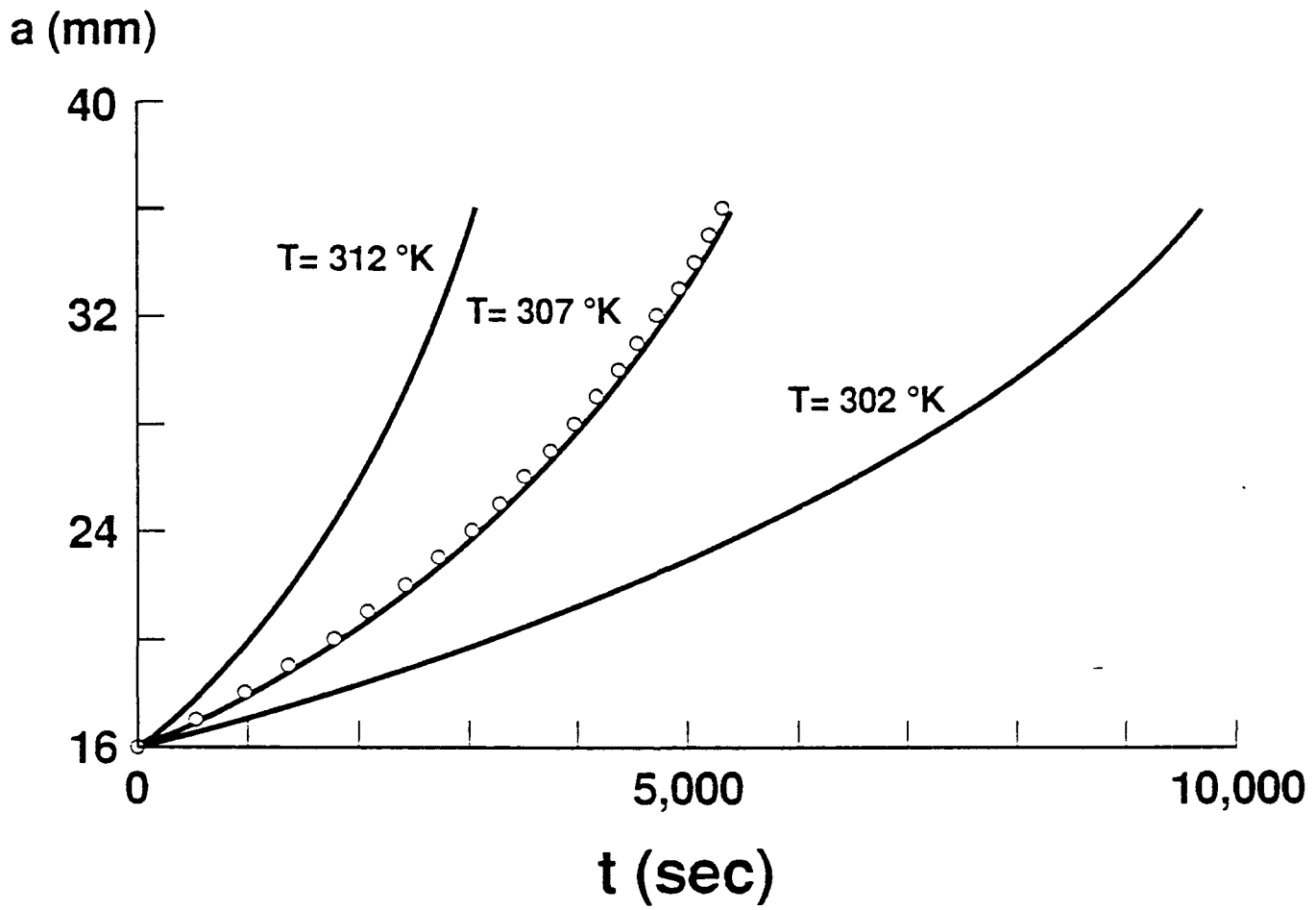

FIG. 6

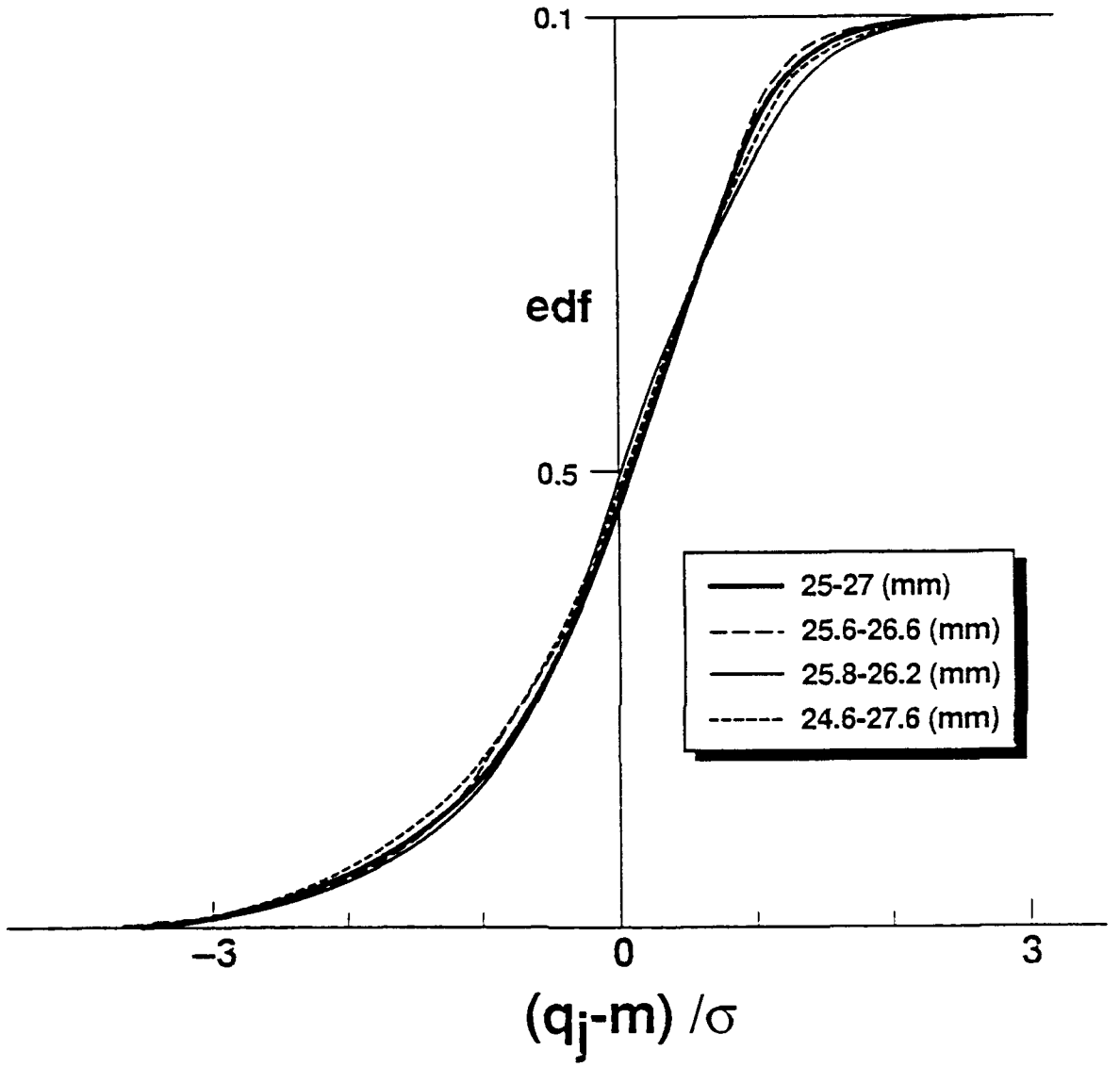
0.1
edf
0.5
25-27 (mm)
25.6-26.6 (mm)
25.8-26.2 (mm)
24.6-27.6 (mm)
−3
0
3
(qj-m) /σ

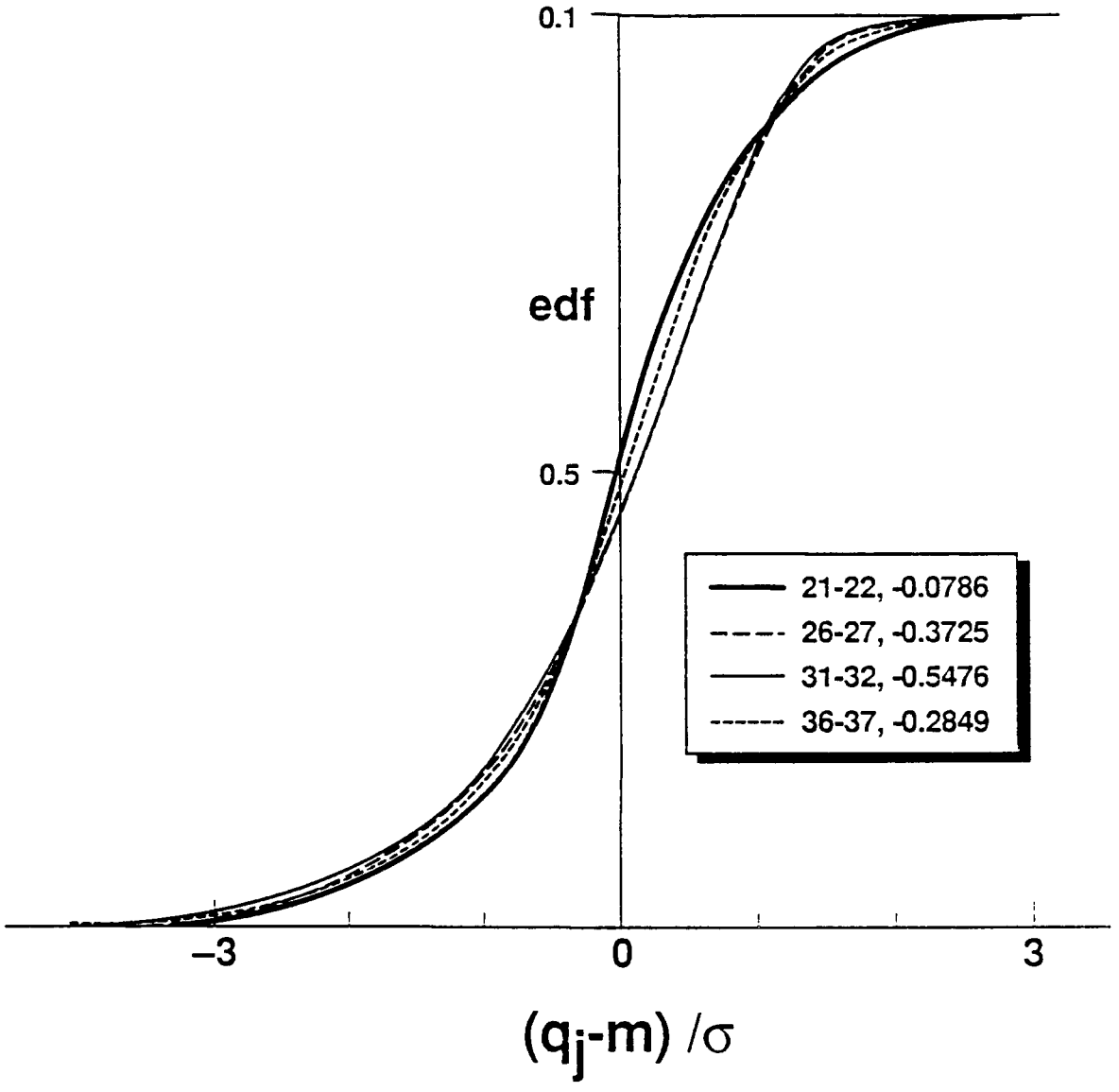
0.1
edf
0.5
21-22, -0.0786
26-27, -0.3725
31-32, -0.5476
36-37, -0.2849
−3
0
3
(qj-m) /σ

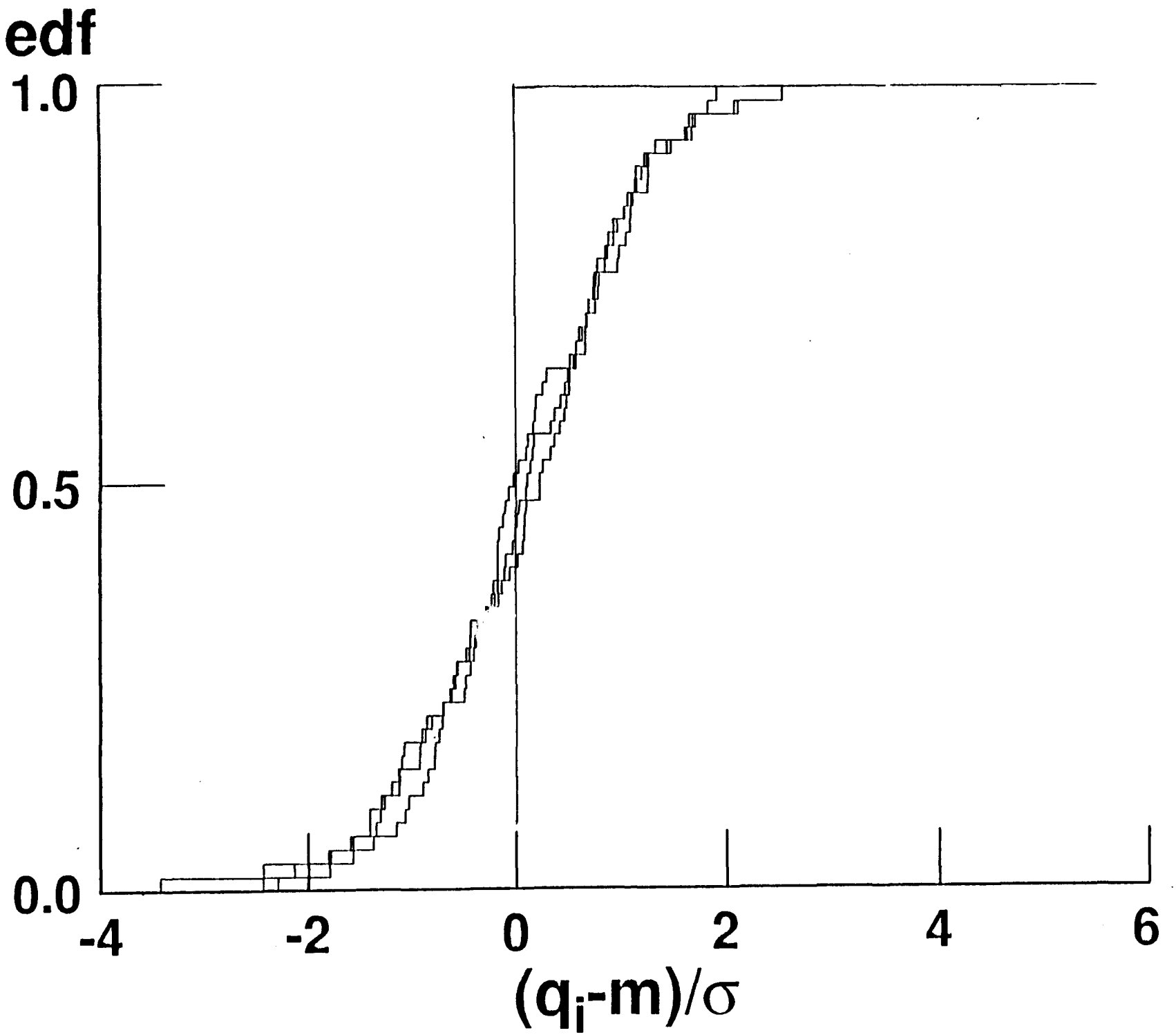

FIG. 10

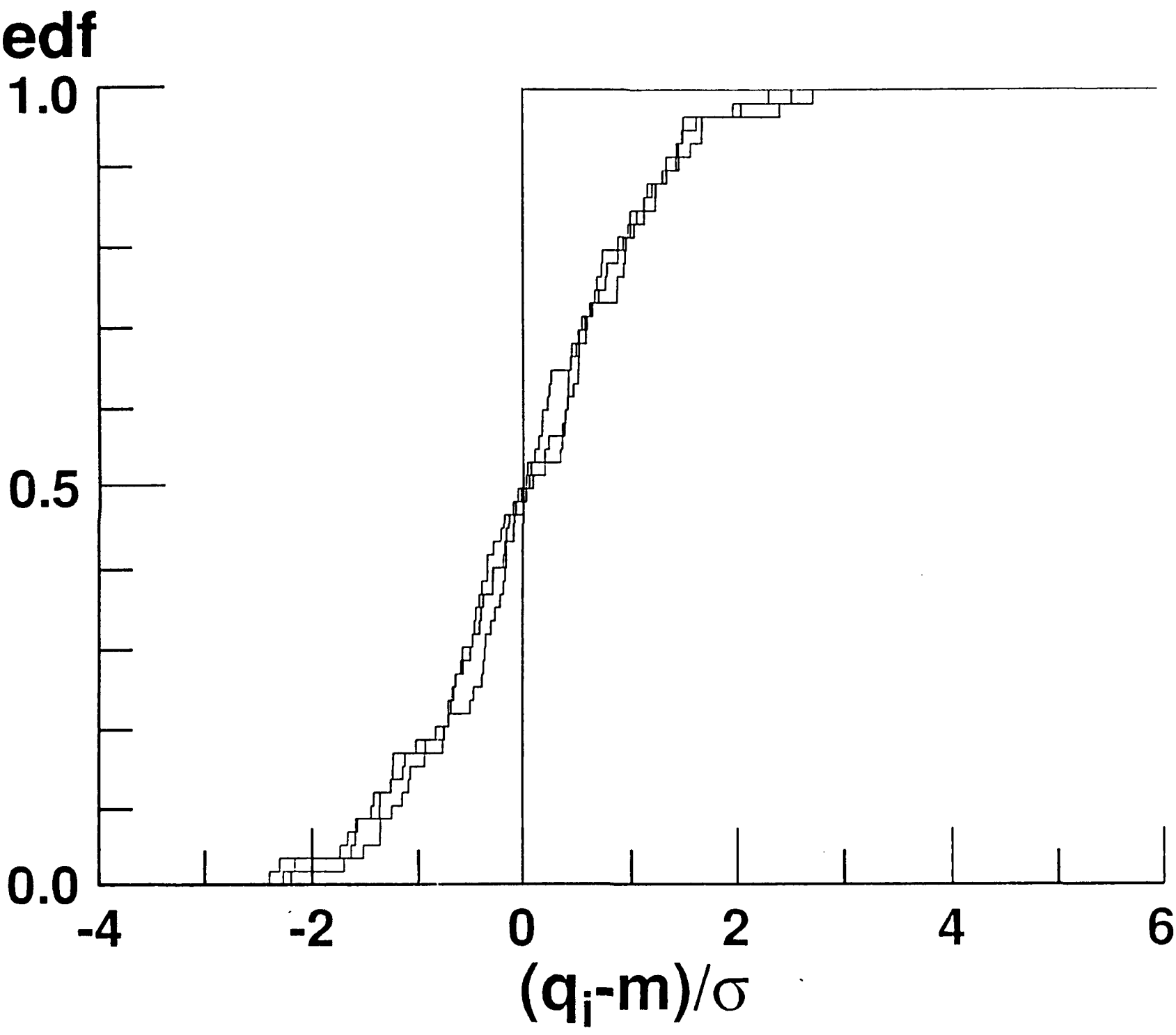

FIG. 11

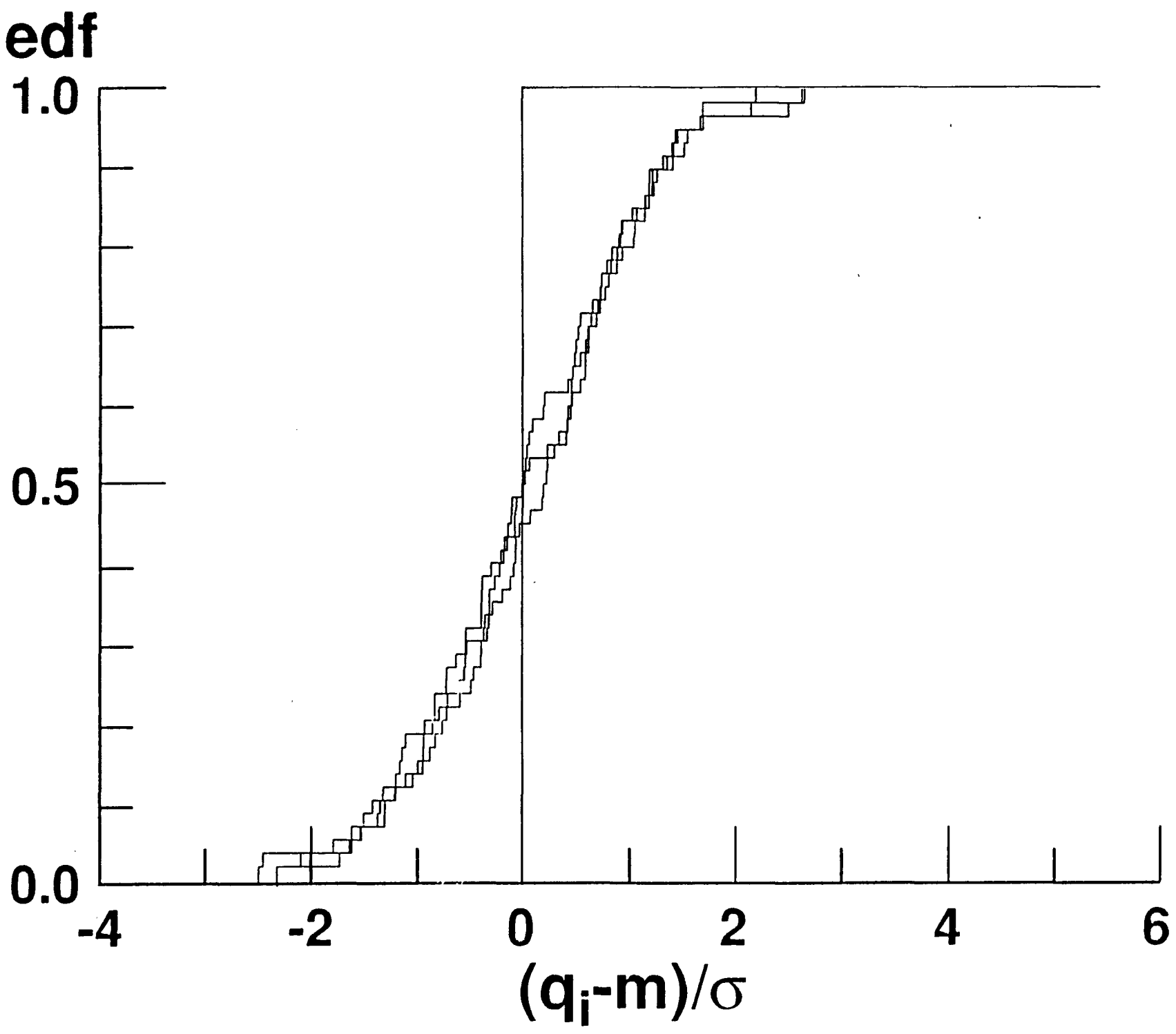

FIG. 12

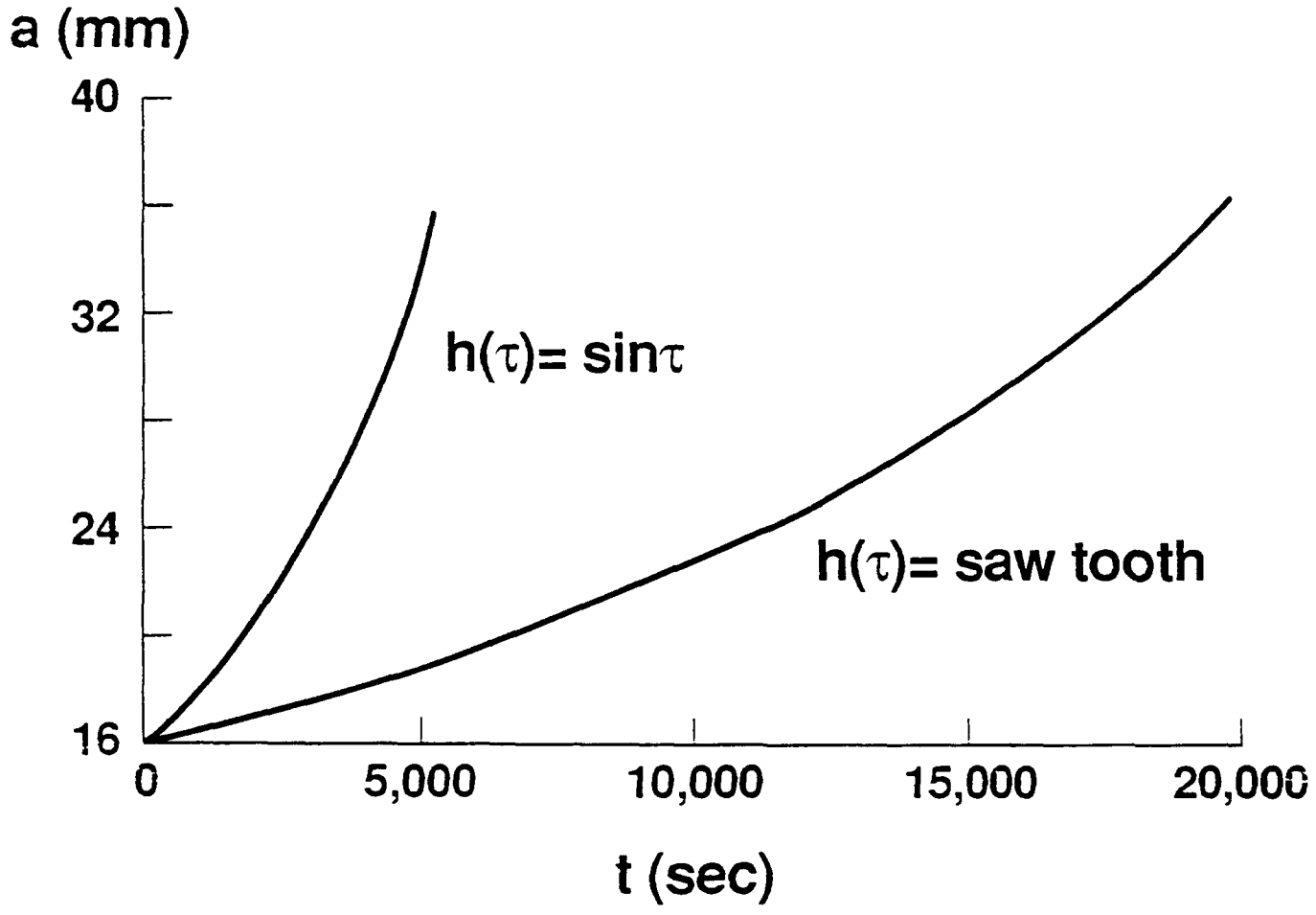
a (mm)
40
32
24
16
h(τ)= sinτ
h(τ)= saw tooth
0
5,000
10,000
15,000
20,000
t (sec)

FIG. 7